A COMPARISON OF GALILEO ELECTRON DENSITY MEASUREMENTS TO A VOYAGER I MODEL IN THE IO PLASMA TORUS

by

Ryan Francis Kadow

A thesis submitted in partial fulfillment of the requirements for the Master of Science degree in Physics in the Graduate College of The University of Iowa

July 2001

Thesis supervisor: Professor Donald A. Gurnett

Graduate College
The University of Iowa
Iowa City, Iowa

CERTIFICATE OF APPROVAL

MASTER'S THESIS

This is to certify that the Master's thesis of

Ryan Francis Kadow

has been approved by the Examining Committee
for the thesis requirement for the Master of Science
degree in Physics at the July 2001 graduation.

Thesis committee: David A. Huntzinger
Thesis supervisor

Gerald Payne
Member

M. D'Angelo
Member

To my mother and father

ABSTRACT

We have inferred electron density values in the Io plasma torus from upper hybrid emissions recorded by the Galileo Plasma Wave Instrument. Comparing the electron density values from the Plasma Wave Instrument to an electron density model which Bagenal has constructed from Voyager I data, we find that the Galileo measurements consistently give larger electron density values from 6-9 R_J. To quantify this difference we have calculated a constant multiple of the model data that minimizes the mean square difference between the observed and predicted density values. For passes J0, I24, I25 and I27 we find that the ratio of the Plasma Wave Instrument electron densities to Voyager I model densities is 1.65. Since the model is derived from Voyager I data our comparison indicates that the plasma density in the Io Plasma Torus is variable by a factor of 1.65 over the past two decades. Electron density variations among individual Galileo orbits suggest that the electron density in the torus may vary by over a factor of two over timescales of tens of years. We have also examined the electron density as a function of latitude from the centrifugal equator to investigate if there are systematic deviations from the Voyager-based model.

TABLE OF CONTENTS

LIST OF FIGURES

INTRODUCTION

History

The first exploration of the Jovian planetary system began in 1610 when Galileo Galilei began observing Jupiter through a telescope of his own construction. He saw Jupiter as no one in history had before, but more importantly he saw four tiny points of light moving about Jupiter. Today we know these points of light as the Galilean moons of Jupiter[i]. This was a crucial observation, for it provided an example of a system which was not geocentric. With Earth not at the center of the Jovian planetary system it was a short step to wonder whether Earth were at the center of the known Solar System. In this sense Galileo's observations become a cornerstone of the Copernican Revolution.

The first hints of the richness and complexity the Jovian system has to offer us came three and a half centuries later in 1955 when Burke and Franklin discovered decametric radio frequencies originating at Jupiter[ii]. This was the first evidence that Jupiter had a magnetic field and it was the first evidence for a magnetosphere anywhere in the Solar System. It was shown ten years later that Io largely controlled these emissions[iii]. This finding established a strong relationship between Io and Jupiter, as well as between Io and Jupiter's magnetosphere. This was in part the motivation that spurred researchers to send satellites to collect in situ measurements of the Jovian system. The era of satellite exploration at Jupiter was begun by Pioneer 10 in 1972 and Pioneer 11 in 1973. Both spacecraft successfully flew

by Jupiter a year after their respective launches making the first in situ measurements of the Jovian system[iv].

In 1976 Earth based observations detected a torus of singly ionized sulfur surrounding Jupiter and radiating in the ultraviolet[v]. Although not widely appreciated at the time this was the first evidence for the existence of a plasma torus around Jupiter. This work was continued in 1977 when NASA launched the two Voyager satellites on their epic mission through the Solar System. Voyager I flew within 5 R_J of Jupiter on 5 March, 1979 and Voyager II flew within 10 R_J of Jupiter four months later[vi]. Both satellites carried a variety of detectors, including plasma and plasma wave instruments[vii]. One of the most important discoveries from the Voyager missions was volcanism on Io. Ironically, this volcanic activity was predicted on theoretical grounds several weeks before it was discovered in Voyager I images[viii]. This provided a link between Io and Jupiter that will be explored more fully in this work. The Voyager missions significantly expanded our knowledge of the plasma properties in the Io plasma torus, as well as the rest of Jupiter's magnetosphere.

Spurred on by the success of the Voyagers, though much delayed by the space shuttle catastrophe, NASA launched the Galileo spacecraft in 1989 and, after an extended trip, it arrived at Jupiter in 1995. Unlike the Pioneers and Voyagers, Galileo has been orbiting Jupiter since its arrival, providing invaluable spatial and temporal coverage of the Jovian system[ix]. The spacecraft carries a suite of nine instruments that have contributed immensely to our understanding of Jupiter's atmosphere, magnetosphere , plasma torus and especially the four Galilean moons. Scientific highlights of the mission include a probe that was dropped into Jupiter's atmosphere, the potential discovery of subsurface, briny oceans on Europa, Ganymede and Callisto and the confirmation of a high altitude ionosphere for Io.

In addition to satellite measurements, researchers have been making valuable observations of the Jupiter system from Earth for the past 5 decades and outstanding research has been done with the Hubble Space Telescope since the early 1990's. In the coming decade NASA has plans for a Europa Orbiter[x] to search for signs of life in the oceans beneath Europa's icy crust.

Jupiter's Magnetosphere

A planetary magnetosphere is the region of space surrounding a planet that contains that planet's magnetic field. Within this region the dynamics of charged particles are controlled primarily by the planet's magnetic field. The dimensions of a planet's magnetosphere are controlled by the supersonic solar wind emanating from the Sun. Solar wind pressure competes with the magnetosphere's magnetic field and particle pressure to determine the magnetosphere's shape and extent. Jupiter's magnetosphere, by virtue of its above average particle pressure, is much larger than was originally expected.

Jupiter's magnetic field can be approximated by an electric dipole and it is offset from the rotation axis by roughly 10°[xi]. Thus, Jupiter has a spin equator and a magnetic equator which are not aligned, just as on the Earth. This complicates the situation somewhat because plasma on a magnetic field line behaves like a bead on a wire. This is a consequence of the frozen field theorem. The rigidly rotating plasma has its lowest energy configuration when it is on the point of the magnetic field line that lies furthest from the planet's rotational axis. The locus of all such points is called the centrifugal equator. In the absence of

electrostatic forces and thermal motion plasma would be confined to the centrifugal equator. Figure 1 shows Jupiter's rotational, centrifugal and magnetic equators.

Of course, plasma cannot corotate at great distances from the planet. The further from the planet the greater the centrifugal forces and the harder it is for the system to maintain corotation. Plasma in the magnetosphere is connected to Jupiter's ionosphere through magnetic field lines. The ionosphere is in turn connected to Jupiter's neutral atmosphere through collisions. The ionosphere/neutral atmosphere connection acts as a clutch that drives corotation. If the corotating plasma puts too great a load on this 'clutch' it will begin to slip and corotation will start to fail. In practice corotation already fails by roughly 1% at Io's orbit, or 6 R_J. At 8-9 R_J plasma rotates 3-5% slower than the planet and at 20 R_J there are substantial deviations from corotation[xii].

Jupiter's magnetosphere is immense. There are three reasons for this: Jupiter's strong magnetic field, the large particle pressure due to Io's volcanism and the feebleness of the solar wind at Jupiter's distance from the Sun. However, as can be seen in figure 2, in its basic construction it is much like the Earth's magnetosphere, the Io plasma torus being the famous exception. The sunward border of Jupiter's magnetosphere is delimited by the bow shock where the solar wind is forced to flow around Jupiter's magnetic field. This point varies between 40 – 100 R_J depending on the solar wind strength. On the anti-sunward side Jupiter's magnetic tail extends far out into interplanetary space, even past the orbit of Saturn. Closer into Jupiter, from roughly 5-10 R_J, the Io plasma torus is the dominant feature. Material from the torus drifts radially into the magnetosphere to form the plasma disk, also called the current sheet, which itself is eventually attenuated in the magnetospheric tail. If there were no mechanism for particles to escape out of the magnetosphere it would grow

without limit. This is clearly not the case so there must be some machinery for removing plasma from the system roughly on the same time scale as it is added. It is generally believed that plasma drifts down the magnetic tail and is eventually lost into interplanetary space.

Io

Io is unique in the Solar System. It is the nearest Galilean moon to Jupiter. It has nearly the same mass as Earth's Moon and nearly the same orbital distance from Jupiter as the Moon has from Earth[xiii]. The similarities cannot be pressed much further however. Io's orbit about Jupiter is slightly elliptical and Io revolves quite rapidly, with a period of 1.8 days. Io is also locked into an orbital resonance with Europa, and the largest moon in the Solar System, Ganymede. The combination of these two orbital characteristics result in varying tidal pressures on the moon, very much the way the Sun and the Moon combine to affect tides on the Earth. The effect is much greater at Io, deforming the moon's crust by 300 feet per orbital period. This results in tremendous thermal heating of the moon's interior which gives rise to spectacular and continuous volcanism. The first evidence for volcanism on Io came from Voyager I images. Since then the Hubble Space Telescope has monitored Io's volcanic activity and this has been studied extensively during the Galileo mission. As a result of its ubiquitous volcanic activity Io has the youngest surface in the Solar System. No impact craters have been found on Io indicating that its crust must be resurfaced on the order of 10^6 years.

Io ejects primarily sulfur and oxygen, but also potassium, sodium and magnesium. These erupted compounds are weakly held by Io's gravity, so volcanic plumes often reach hundreds of kilometers into space. Once aloft, the ejected compounds have a very good chance of being able to escape into space. If they fall back to the surface they contribute to Io's wildly mottled hue of orange, white, yellow and black. If they escape from the moon, however, they have a much more interesting life cycle.

By virtue of the many particles that do stay aloft after ejection, Io can be said, in a very loose sense, to have an atmosphere. This atmosphere would be a good vacuum in an Earth-bound laboratory. It is not continuous like the Earth's atmosphere but patchy, being found primarily around active vents and volcanoes. Around such regions sulfur column densities of $10^{15} - 10^{17}$ particles cm^{-2} have been measured[xiv]. On the other hand, in volcanically inactive regions sputtering or sublimation may be the only processes contributing to the atmosphere and it is then all but non-existent.

A particle in Io's atmosphere has a good chance of being ionized through electron impact or photoionization. As a neutral it shares its orbital speed with Io, roughly 17 km/s. Once the particle is ionized, however, it feels Jupiter's magnetic field sweeping by it at a relative speed of 57 km/s. The resulting Lorentz force picks up the ion or electron and accelerates it until it is corotating with Jupiter. Thus, Jupiter's rotational energy, for all practical purposes an infinite reservoir, is the source that gets tapped to energize magnetospheric plasma. Through this pickup mechanism Io adds roughly one ton of material every second to the Io plasma torus[xv].

Structure of the Io Plasma Torus

The Io plasma torus consists of roughly two million tons of oxygen and sulfur in various charge states arranged like a doughnut around Jupiter[xvi]. A cross section can be seen in figure 3. This torus can be divided into two broad regions, the cold torus and the warm torus, each with its own unique properties, separated by a distinct border.

Nearest to Jupiter, inside the orbit of Io, is the cold torus. Electrons in this region have energies on the order of a few eV[xvii]. Collision rates are much higher in the cold torus than the warm torus. The proposed mechanism for cooling these electrons after they are picked up by the magnetosphere is radiation. Electrons drift into the cold torus more slowly than into the warm torus. This gives them more time to radiate and cool. As they loose energy they collapse onto the centrifugal equator. This results in an increased electron density which promotes further radiation which compounds the effect. The scale height is relatively small in the cold torus, about 0.2 R_J, which leads to significant uncertainties in modeling the plasma parameters. For this reason we have not included the region of the cold torus in this study.

The region from Io's orbit to approximately 10 R_J is called the warm torus. The scale height is about 1 R_J in the warm torus. There are two electron populations in the warm torus: moderately energetic electrons which have a maxwellian distribution and a smaller, non-maxwellian component of suprathermal electrons with higher energies. As one moves away from Jupiter the ratio of suprathermal to thermal electrons increases from about 0.02% to a maximum of 8% in the outer region of the torus[xviii]. Figure 4 shows two features, called the ledge and the ramp, which have been identified in the warm torus. The ledge extends from

6-7 R_J and displays only small variations of electron density with radial distance. The ramp, from 7-8 R_J, exhibits a more severe drop-off in the electron density. Beyond 8 R_J the torus gradually diffuses into the plasma disk. In this region plasma corotation begins to fail.

PLASMA THEORY

A plasma consists of atoms or molecules in assorted charge states that are connected to each other through Coulomb potentials. The particles in a plasma exhibit collective behavior when there are a large enough number of particles. The Debye length determines what is a 'large enough' number of particles. Debye length is given as:

$$\lambda_D = \sqrt{\frac{kT_e\varepsilon_0}{n_e q_e^2}}$$

where k is Boltzman's constant, T_e, n_e, q_e are the electron temperature, number density and charge respectively and ε_0 is the dielectric constant in free space. While there must be charge separation for the plasma to exist, the plasma taken as a whole will be neutral on scales larger than the Debye length. Thus, if the condition:

$$N_D = n_e 4/3\pi\lambda_D^3 >> 1$$

is satisfied, the plasma will exhibit collective behavior and can be treated as a fluid. Plasmas turn out to be more complicated than regular fluids, such as oceans or atmospheres, because of the electric and magnetic fields involved. However, just as waves propagate through fluids there are many different wave types that propagate in plasmas[xix]. For this study the upper hybrid frequency is particularly important. Upper hybrid waves are high frequency, electrostatic electron oscillations perpendicular to a zeroth order magnetic field. This is laid out schematically in figure 5. The important points to note are that it is primarily the electrons that move, one assumes that the ions are too massive to respond to the high

frequency driving force, and the oscillations are of a high frequency[xx]. Mathematically, the upper hybrid frequency is a combination of two frequencies:

$$f_{UH}^2 = f_P^2 + f_C^2$$

f_p is the plasma frequency:

$$f_P^2 = \frac{e^2 n_e}{m_e \varepsilon_0} \approx 8980 * \sqrt{n_e} \text{ Hz}$$

The important point is that the plasma frequency carries information about n_e, the electron density. The other parameters are the electron charge, electron mass and permittivity of free space.

The second component, f_c, is the cyclotron frequency:

$$f_c = \frac{eB}{m_e} \approx 28B \text{ Tesla}$$

The cyclotron frequency carries information about the magnetic field strength. Galileo also carries a magnetometer that directly measures Jupiter's magnetic field. In our work the cyclotron frequency is generally an order of magnitude smaller than the plasma frequency and can be ignored as a secondary effect. Thus, by measuring the upper hybrid frequency we are essentially measuring the plasma frequency which is a direct and accurate indicator of the electron density.

GALILEO'S PLASMA WAVE INSTRUMENT

After extensive delays NASA launched the Galileo spacecraft in 1989. Following an extended tour of the inner Solar System, including flybys of Earth (where signs of life were detected) and Venus (where signs of lightning were detected) Galileo went into Jovian orbit in 1995. Galileo carries numerous instruments, including the Plasma Wave Instrument designed to detect plasma waves and radio emissions in the Jovian Magnetosphere[xxi]. The plasma instrument consists of an electric dipole antenna, two search coil magnetic antennas plus instrumentation. Since the search coil magnetic antennas are not used to detect upper hybrid waves (upper hybrid waves are electrostatic waves) it will not be described here. The electric dipole antenna is roughly 6.5 meters long. Shown in figure 6, it is mounted at the end of the spacecraft's magnetometer boom perpendicular to the boom to lessen the effect of unwanted electric field signals from the spacecraft. The frequency range of this instrument is 5.6 Hz to 5.6 MHz. Although three frequency analyzers are used, the upper hybrid frequency signals used in this study all fall in the range of the highest frequency spectrum analyzer. This instrument monitors 42 frequencies in the range of 100 kHz to 5.6 MHz. The frequency interval ($\Delta f/f$) is roughly 10%. The bandwidth is 1.3 kHz, the dynamic range is 100db. It takes 18.67 seconds to complete a full spectral sweep. The time required for a full electric and magnetic spectral sweep is twice as long, 37.33 seconds.

Data from the Plasma Wave Instrument is presented in the form of a spectrogram. Examples of spectrograms can be seen in figure 17. The ordinate is

frequency and the abscissa is time, Jovian radii, system three longitude, and magnetic latitude. Color indicates signal strength. Many different plasma waves and radio emissions can be seen on a spectrogram. One can plot time intervals varying from minutes to days. There are several minor interference signals at high frequency. Since they stay at a single frequency in time they are easily distinguished from upper hybrid signals which tend to vary in time as the electron density rises and falls. Fortunately, the upper hybrid wavelengths we measure are much larger than the spacecraft (typically hundreds of meters) so differential charging and shielding effects from the spacecraft do not pose a problem.

1994 BAGENAL MODEL

The radial and latitudinal structure of the Io plasma torus has been modeled by Bagenal using Voyager I plasma data[xxii]. We used this model extensively in this study so I will briefly describe it in this section.

In March, 1979 Voyager I flew within 5 R_J of Jupiter. This trajectory took it through the Io plasma torus on both the inbound and outbound orbits and the Plasma Science and Ultraviolet Spectrometer instruments onboard made in situ and remote observations of the plasma respectively. Using the data along Voyager's trajectory as a starting point the model was created by numerically solving the equations of diffusive equilibrium to create radial and latitudinal profiles for electrons and thirteen ion species.

The idea is that an electron on a magnetic field line feels several forces: a net electric force from electrons and ions on the centrifugal equator, a centrifugal force from its rotational motion and a thermal pressure that will move it along the field line[xxiii] . Eventually an force equilibrium is reached. This is what has been modeled. A radial profile for electrons can be seen in figure 7.

The distribution of electrons along a magnetic field line depends primarily on the component of the electron temperature along that field line, $T_{\parallel}$. Unfortunately, Voyager I only measured $T_{\perp}$. To overcome this it is assumed that the electrons, both the thermal and suprathermal populations, are isotropic. This is probably a reasonable assumption for thermal electrons. Timescales for radial transport of plasma varies between 1-10 days[xxiv]and

80-150 days[xxv]. Typical timescales for electrons to reach isotropy through collisions vary between five minutes for cold electrons (~ 5 eV) to two days for hot electrons (~ 400 eV)[xxvi].

One of the complications confronting this model is the difficulty in separating radial density variations from latitudinal density variations. Outside of Io's orbit, electron density decreases with increasing radial distance. Electron density also decreases with increasing latitude as measured from the centrifugal equator. The scale height associated with this attenuation is 1 R_J in the warm torus. Because the model is built on a single trajectory it is difficult to distinguish between radial and latitudinal effects. Furthermore, longitudinal variations in the plasma torus have been observed[xxvii] but it is impossible for the model to distinguish between radial and longitudinal variations based on the data from a single trajectory. Thus, longitudinal variations are not considered. It is also assumed that the timescales in the torus are larger than the time it took Voyager I to pass through the torus.

The model is not very accurate inside 5 R_J because the results start to depend heavily on the magnetic field model that is used. Also, outside of 8 R_J, the current sheet, or plasma disk, begins to perturb the magnetic field and has the effect of flattening the radial density profiles. Given this, the model claims to provide a reasonable picture of the torus between 5-10 R_J.

METHOD

The goal of this project is to compare electron density values from Galileo's plasma wave instrument to electron density values predicted by the Voyager I model. These values are not in agreement and we have characterized the differences by finding a constant value that minimizes the least square difference between them. We adjusted the model by this constant value and then looked for additional discrepancies between the two data sets. We first considered electron density as a function of radial distance. We have also checked for systematic electron density variations as a function of latitude.

Galileo has completed 30 orbits as of this writing. Six of the orbits have been chosen for analysis. We have used the J0, I24, I25, I27[xxviii] orbits to make a radial comparison and the C23 and G29 orbits to make a latitudinal comparison. The first four orbits were chosen because they penetrated sufficiently deep into the Io plasma torus. The latter two were chosen because they showed electron density variations with magnetic latitude. Galileo's trajectory for the first four orbits is plotted over a model-generated electron density map in figure 8. We have restricted our study between the radial distances of 6-9 R_J. Inside 6 R_J the scale height in the cold torus is very small and as a result the model uncertainty is quite large. Outside 9 R_J the upper hybrid signal becomes to weak too measure as the electron density decreases, and the model begins to suffer from magnetic perturbations from the current sheet.

The first step in analyzing the electron density is to identify the upper hybrid frequency. This is done using a power vs. frequency plot (see figure 9). The Plasma Wave

Instrument generates one such plot every 37.33 seconds. Generally, one goes about this by selecting an orbit and then looking at the perijove portion of that orbit[xxix]. On a spectrogram the upper hybrid frequency will be clearly visible, typically for several hours. By comparing the power vs. frequency plot with a spectrogram one can identify the upper hybrid frequency on the former plot. Working with the power vs. frequency plot one then takes a short segment, perhaps 30 minutes in length, and beginning at t=0 identifies the upper hybrid frequency. To do this a cross-hair is lined up at the appropriate frequency and a mouse-click tells the computer program to label that frequency as the upper hybrid frequency. One is then provided the next plot which was generated by the Plasma Wave Instrument 37.33 seconds later. By repeating this process one moves forward in time at discrete 37.33 second intervals until the entire upper hybrid signal has been digitized for that pass.

There can be some uncertainty in this process depending on the shape of the upper hybrid signal. Ideally, the upper hybrid peak would be confined to a single frequency and it would stand out well above the background noise threshold. Of course this ideal situation is never realized. The actual signal one must work with may have a number of distortions:

1) The peak may be asymmetrical

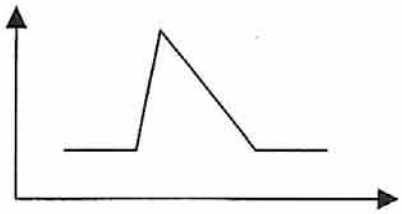

2) The peak may be wide

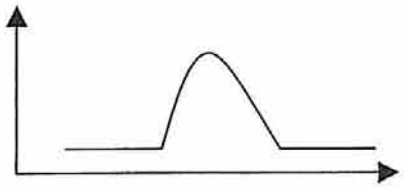

3) The signal may not present a peak at all

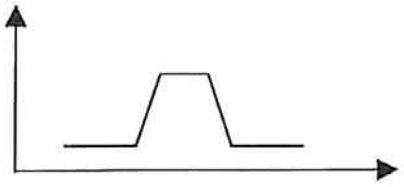

4) There may be multiple peaks

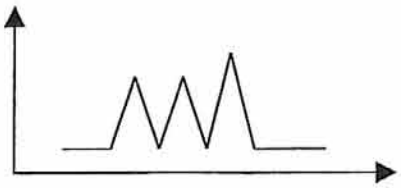

5) The peak my not stand out above the noise threshold

These problems are addressed in a qualitative fashion by assigning to each upper hybrid frequency data point a number called its quality factor. The quality factor represents the researchers confidence that the frequency they picked is indeed the upper hybrid frequency. The number 0 represents the highest confidence rating, the number 4 represents the lowest confidence rating with numbers 1 and 2 designating a middle ground. This is a subjective analysis. Given enough time at the computer each worker tends to establish criteria in their own mind for assigning their confidence ratings. Thus, while the initial ratings may be somewhat erratic, over time one settles into a solid pattern. All the orbits used in this study were digitized by the same person.

A second complication that can occur arises from the users ability to place the mouse cursor on exactly the right pixel and not to move it when they click the mouse. There is an undeniable human element implicit in this analysis. Ultimately, the processed signal is always checked against the spectrogram so that any flagrant violations will be caught. More subtle variations tend not to be important since we are looking at broad trends in time and space rather than minute to minute differences.

There is a certain amount of ambiguity in the spectrogram as to the exact location of the upper hybrid frequency. Referring to the spectrogram for pass C23 in figure 17 as an example it is very clear that the upper hybrid frequency is not confined to a single frequency. Rather it is spread out over a band of frequencies. In order to characterize this uncertainty in the upper hybrid frequency error bars have been overlaid on the radial density plot for orbit I24 (see figures 10). The lower bound on the error bar corresponds to the lower bound of the upper hybrid signal and the upper bound on the error bar corresponds to the upper portion of the upper hybrid signal. It is reasonable to expect that the true upper hybrid frequency must lie within these two boundaries and this expectation is born out in the density plots.

With the Plasma Wave Instrument data digitized, the next step was to find a constant value that would characterize the difference between the measured electron densities and the model electron densities. For orbits J0, I24, I25 and I27 we multiplied the model electron density by an incrementing series of numbers between 1 and 2 to find a value which minimized the least square difference between the two data sets. This value turned out to be 1.65. We then multiplied the model electron densities by 1.65 and calculated the difference between the Plasma Wave Instrument electron density and the model electron density by:

$$\text{Log (Galileo } n_e \text{) – Log (Model } n_e \text{ * 1.65)}$$

Using the property of logarithms,

$$\log A - \log B = \log \frac{A}{B}$$

the above statement is equivalent to

$$\text{Log (Galileo } n_e \text{ / Model } n_e \text{ * 1.65)}$$

This quantity is on the ordinate in figures 11 – 16, 18 and 19. In doing this we have found density features that are potentially radially dependent.

RESULTS

For orbits J0, I24, I25 and I27 the plasma wave instrument found larger electron densities than the Voyager I model predicted. Minimizing the least square difference for those four orbits simultaneously yielded a value of 1.65. A pass by pass analysis suggests that the electron density in the Io plasma torus can vary by a factor of two or more.

J0

On July 12, 1995 Galileo went through the perijove point of its insertion orbit. The spacecraft passed very near to the planet, coming within 4.5 R_J. A large data gap has restricted the radial comparison to the region between 6.0-7.7 R_J of the inbound pass. There was no data taken on the outbound pass. The Plasma Wave Instrument found much higher electron densities than had been predicted. The constant value that minimizes the least mean square for this pass alone is 2.3.

Following the analysis routine described in the Method section, we increased the model electron density by 1.65 and then used the log property to look at the remaining differences. This is plotted in figure 11[xxx]. If increasing the model electron density by 1.65 matched the model electron density perfectly to the Plasma Wave Instrument electron density this plot would be a horizontal line at 0 on the y axis. In fact the entire line is above the zero mark indicating the electron density was above average even after increasing the model

electron density by 1.65. There are peaks at 6.5 and especially 7.5 R_J. Referring to the Galileo trajectory plot in figure 8 these peaks came when the spacecraft was 0.3 and 0.6 R_J above the centrifugal plane respectively.

These features are ubiquitous in our analysis and may demonstrate that electron density does not vary smoothly with radial distance. Electrons evidently prefer to clump together, leaving gaps in between. These features tend to appear outside of 7 R_J and are not as common nearer the planet.

I24

On October 10, 1999 Galileo went through the perijove point of its 24th orbit. A clear upper hybrid signal was detected from inside 6 R_J out to nearly 9 R_J on the outbound pass. As always the Plasma Wave Instrument found a higher electron density than was predicted. The constant value that minimizes the least mean square for this pass alone is 1.45

In the I24 density plot, figure 12 , two features clearly stand out at 7.5 and 8.25 R_J. These occurred 0.9 and 0.8 R_J above the centrifugal equator respectively. These density features are showing up on length scales of ~0.5 R_J.

I25

On November 25, 1999 Galileo went through the perijove point of its 25th orbit. An upper hybrid signal was detected from 6-9 R_J on the inbound and outbound passes. The constant values that minimize the least mean square for the inbound and outbound passes

respectively are 1.43 and 1.44. There are clear density features on both passes (figures 13 and 14). On the inbound pass there is a large density peak at 8 R_J with a density trough at 8.5 R_J followed by a second peak at 9 R_J. These occur at 0.1, 0.7, and 1.1 R_J above the centrifugal equator respectively. Further in at 7.25 R_J there is a smaller peak 0.4 R_J beneath the centrifugal equator.

The outbound pass is almost a mirror image of the inbound pass. There is a peak at 7.75 R_J and 8.5 R_J with a density trough separating them at 8 R_J. These occur at 0.3 R_J above the centrifugal equator, 0.6 R_J beneath the centrifugal equator and 0.1 R_J beneath the centrifugal equator. The length scale for these features is again ~0.5 R_J.

I27

On February 22, 2000 Galileo went through the perijove point of its 27th orbit. The Plasma Wave Instrument collected data from 6-9 R_J on the inbound and outbound portions of this orbit. The constant values that minimize the least mean square for the inbound and outbound passes respectively are 1.38 and 1.83. Density ratio plots for the inbound and outbound pass are in figures 15 and 16.

The inbound plot has a density peak at 7.6 R_J, 0.4 R_J above the centrifugal equator. The outbound orbit presents more of a broad hump than individual peaks. There is a deep trough at 6 R_J which then climbs to a maximum at 7.5 R_J. During this time the spacecraft went from 0.4 R_J beneath the centrifugal equator to its maximum height of 0.8 R_J above the centrifugal equator.

C23 and G29

The perijove sections for the C23 and G29 orbits occurred on September 13, 1999 and December 28, 2000 respectively. These orbits were chosen for analysis because their upper hybrid signals showed clear variations with magnetic latitude as can be seen in figure17. The procedure is exactly the same but now the abscissa is magnetic latitude rather than Jovian radii.

If there were no latitudinally dependent variations between the Plasma Wave Instrument density values and the model density values the plots in figures 18 and 19 would show a horizontal line centered on the ordinate zero. This is very nearly what the G29 orbit shows suggesting that, at least for this orbit, the model densities were quite accurate, within the constant factor, over a range of latitudes. The C23 orbit tends to wander somewhat more from a strict line, yet it is still quite flat and there are no obvious features that would suggest a systematic deviation of electron density with latitude.

DISCUSSION

The clear question is how to interpret the density features that are evident in many of these passes. Taken at face value they can be called regions of higher density that are propagating radially away from the torus under the interchange instability. This is not improbable if one considers Io as the plasma source. Eruptions on Io are probably more discrete than continuous. The moon will eject material in bursts separated by periods of geologic inactivity. The ejected material will be ionized and will propagate away from the torus as clumps of material via the interchange instability. There are no obvious mechanisms that would take an initially clumpy electron distribution and smoothen it.

The majority of these features (11 of 13) have been found outside 7 R_J. This is the region where plasma corotation begins to fail, signaling that the centrifugal forces that would move plasma away from the planet are overcoming the neutral atmosphere/ionosphere clutch mechanism that maintains corotation. This dynamic is consistent with the centrifugally driven flux tube transport hypothesis or interchange instability. In this scenario one assumes the fluid, in this case plasma, is incompressible and analyzes the energy shift that occurs by interchanging two adjacent flux tubes. If the magnetic field lines are concave facing the planet, as they are in planetary magnetospheres, then the flux tube system is unstable and the flux tubes can exchange places. This mechanism allows flux tubes deeper in the torus that are heavily loaded with plasma to exchange places with adjacent flux tubes further out in the

torus that aren't carrying as much plasma. These flux tubes are discrete objects and may explain the electron density features in this study.

Another explanation for these features involves the temperature of the electrons. If the electrons are hotter than the model predicts they will move farther along the magnetic field lines than expected. Conversely, if they are cooler than predicted they will be found closer to the centrifugal equator than expected. For example, if Galileo flies 0.5 R_J above the centrifugal equator and the electrons are hotter than predicted then the Plasma Wave Instrument will find a greater density of electrons than the model predicts and this would look like a higher density feature when the two are compared. If the electrons are hotter than the model allows for they will be found in greater concentrations away from the centrifugal equator and in smaller concentrations at the centrifugal equator. In that case we would expect to see density peaks at larger latitudes and density troughs nearer the centrifugal equator. If the electrons are cooler than the model allows for the trend should be reversed. The data do not clearly support either scenario suggesting that temperature variations are not the primary influence giving rise to the observed density features.

Between 8 and 9 R_J the magnetic field is perturbed by the current sheet. This has the effect of stretching, or flattening the model electron density predictions. This may partially account for the discrepancies in this region, but it should not affect the model inside of 8 R_J. Thus, model distortions due to current sheet magnetic perturbations do not explain electron density concentrations from 6-8 R_J.

CONCLUSION

We have found that the ratio of the Plasma Wave Instrument electron density to the electron density predicted by the Voyager I model to be 1.65. This suggests that the electron density in the torus is dynamic, but relatively stable over a period of decades. Data from four orbits indicate that the electron density in the torus is variable by up to a factor of two on a timescale of years. After increasing the model electron densities by 1.65 we have found strong density gradients on 0.5 R_J distance scales. These density features are interpreted as flux tubes that propagate radially away from the torus via the interchange instability. We have found no compelling evidence for consistent or systematic variations between the measured electron density and the predicted electron density as a function of latitude.

FIGURE 1. Jupiter's Three Equators.

The important point to take from this diagram is that Jupiter has three natural equators: the rotational equator defined by the spin axis, the magnetic equator defined by the magnetic axis and the centrifugal equator defined by the locus of all points on magnetic field lines that are furthest from Jupiter's rotational axis. The centrifugal equator is the minimum energy point for plasma rotating in Jupiter's magnetosphere.

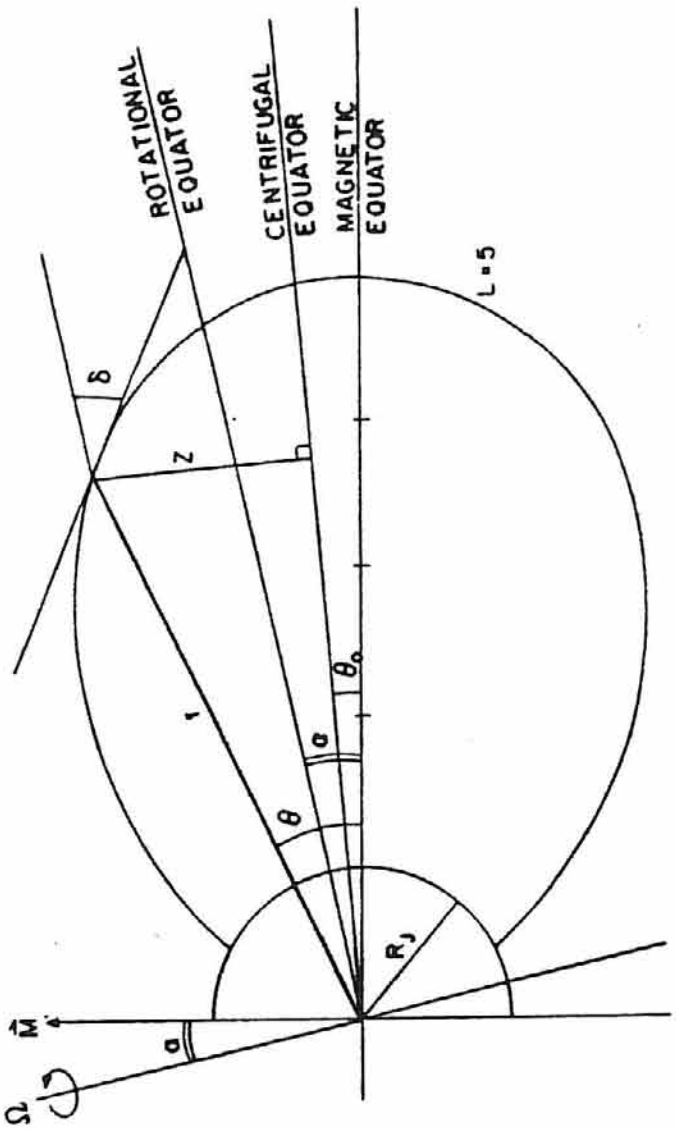
ROTATIONAL EQUATOR
CENTRIFUGAL EQUATOR
MAGNETIC EQUATOR
L=5
δ
z
r
θ
α
θ₀
R_J
M̂
Ω

FIGURE 2. Jupiter's Magnetosphere

The main components of Jupiter's magnetosphere are also common to Earth's magnetosphere, with the exception of the Io Plasma Torus.

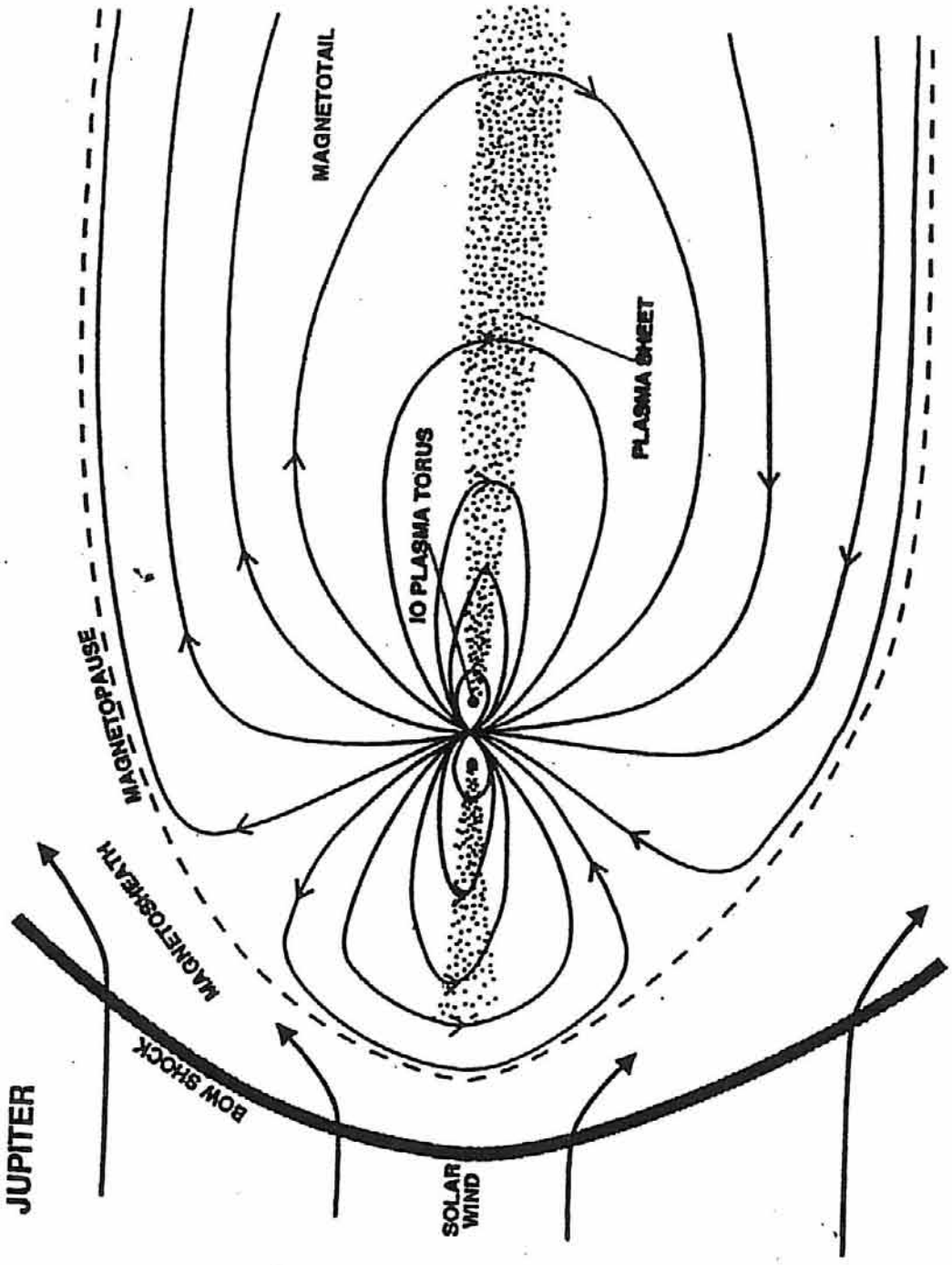
JUPITER
BOW SHOCK
MAGNETOSHEATH
MAGNETOPAUSE
MAGNETOTAIL
IO PLASMA TORUS
PLASMA SHEET
SOLAR WIND

FIGURE 3 Cross-section of the Io Plasma Torus

The important point to take from this diagram is that the torus has two components: the cold torus inside Io's orbit and the warm torus outside Io's orbit. Radial diffusion channels plasma from the warm torus into the plasma sheet.

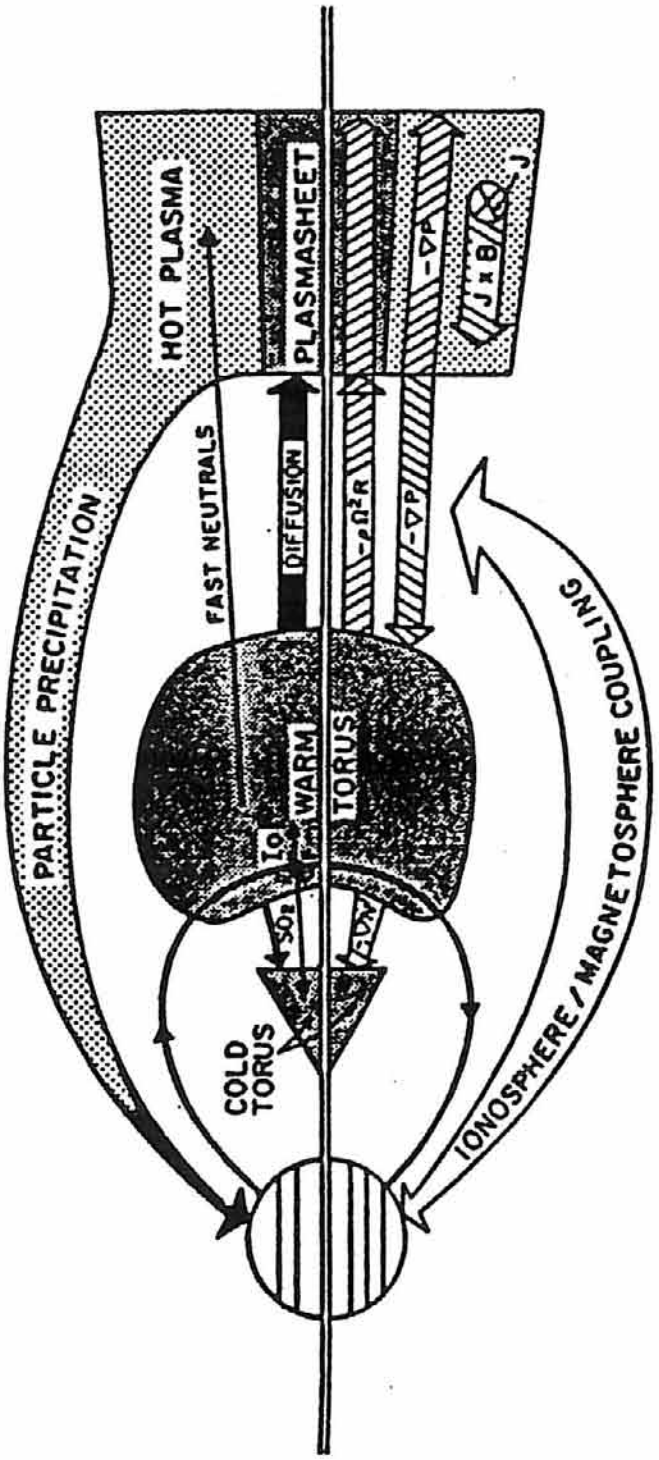
HOT PLASMA
PLASMASHEET
J x B
-∇P
J
FAST NEUTRALS
DIFFUSION
-ρΩ²R
-∇P
PARTICLE PRECIPITATION
IONOSPHERE / MAGNETOSPHERE COUPLING
Io
WARM TORUS
SO2
SUN
COLD TORUS

FIGURE 4. The Ledge and Ramp

If one considers the electron density, or in this graph total flux tube content, as a function of radial distance in the Io Plasma Torus three general regions can be defined. The Precipice is the border between the cold torus and the warm torus. The Ledge is a region of gradually declining electron density in the warm torus. The Ramp is a region of steeply declining electron density in the warm torus.

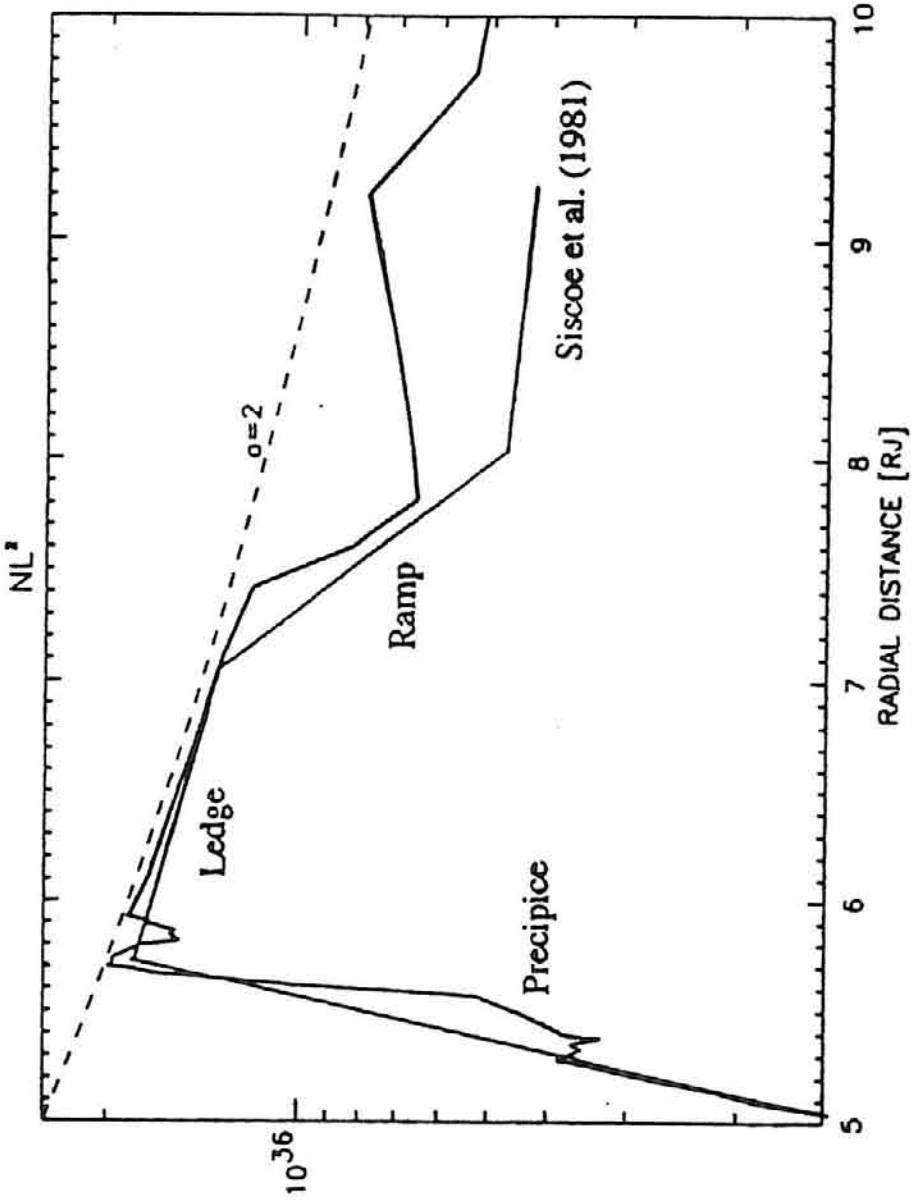
NL²
10³⁶
5
6
7
8
9
10
RADIAL DISTANCE [RJ]
σ=2
Ledge
Ramp
Precipice
Siscoe et al. (1981)

FIGURE 5. Geometry of the Upper Hybrid Wave

The upper hybrid wave propagates along the direction of the oscillating electric field that results from the electrons oscillating about the ions and perpendicular to the direction of the undisturbed magnetic field.

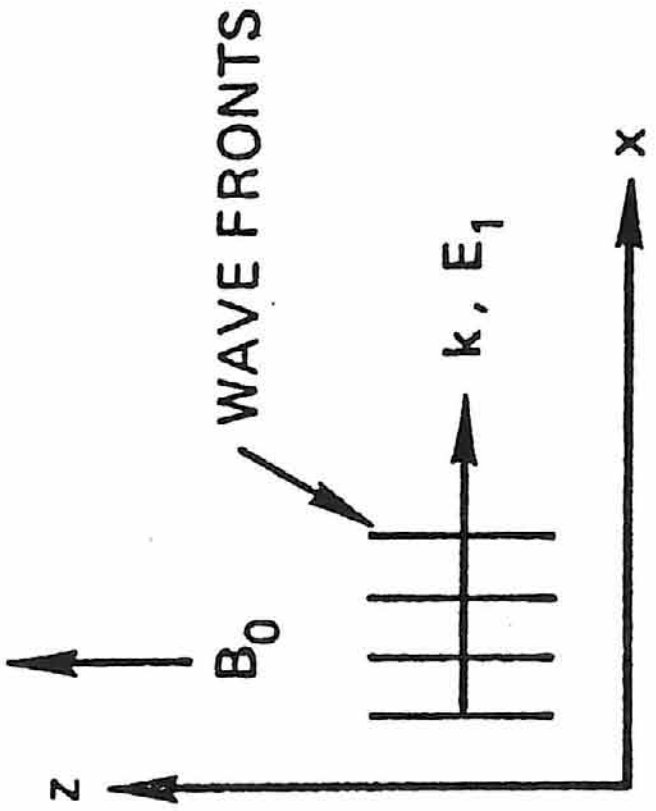

Geometry of a longitudinal plane wave propagating at right angles to B_o.

FIGURE 6. The Galileo Spacecraft

The electric dipole antenna portion of the Plasma Wave Instrument is mounted at the end of, and perpendicular to, Galileo's magnetometer boom.

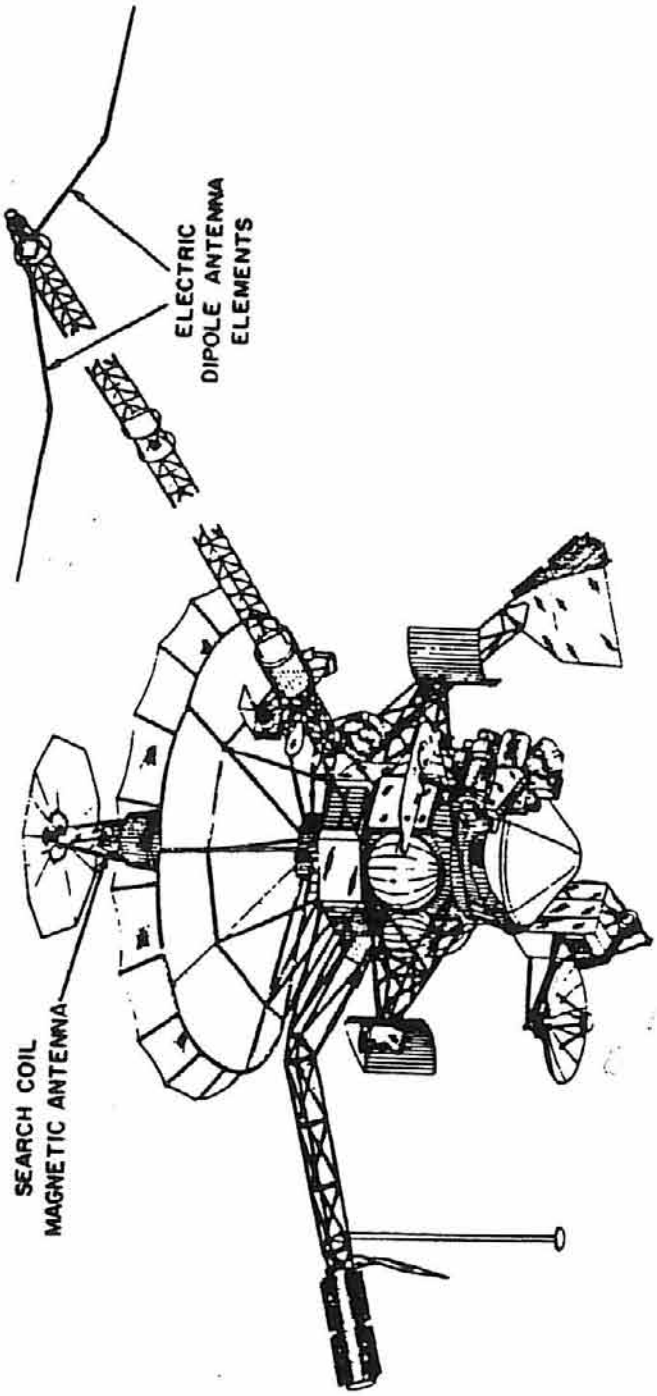
ELECTRIC
DIPOLE ANTENNA
ELEMENTS
SEARCH COIL
MAGNETIC ANTENNA

FIGURE 7. Model Generated Electron Density Profile

This is a two-dimensional electron density profile generated by Bagenal's 1994 Voyager I model at 292 ° in the meridional plane. At 292° System III longitude the rotational, magnetic and centrifugal equators all coincide. The ordinate is in R_J. Contour levels are scaled by factors of 2.

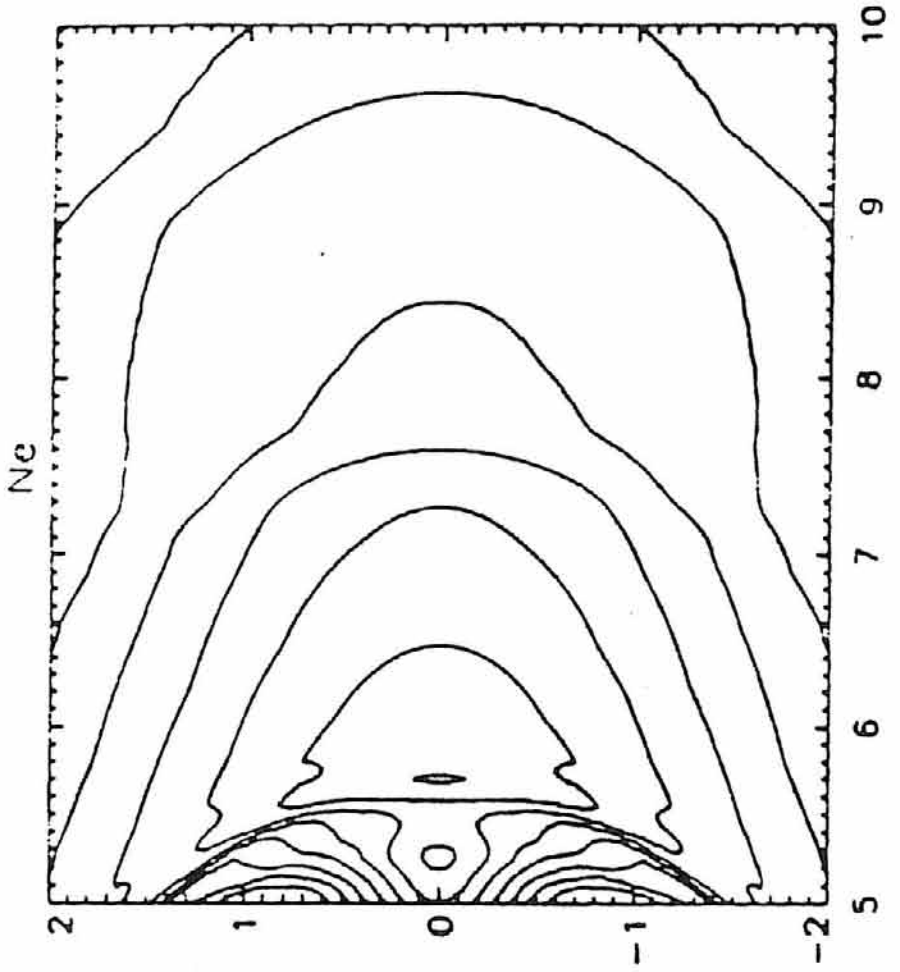
Ne
2
1
0
−1
−2
5
6
7
8
9
10

FIGURE 8. Galileo's Trajectory Superimposed over an Electron Density Map

The electron density map is analogous to the one in figure 7. The trajectories of four of the Galileo orbits used in this study have been traced over the electron density map. The arrows indicate the direction of the inbound orbit.

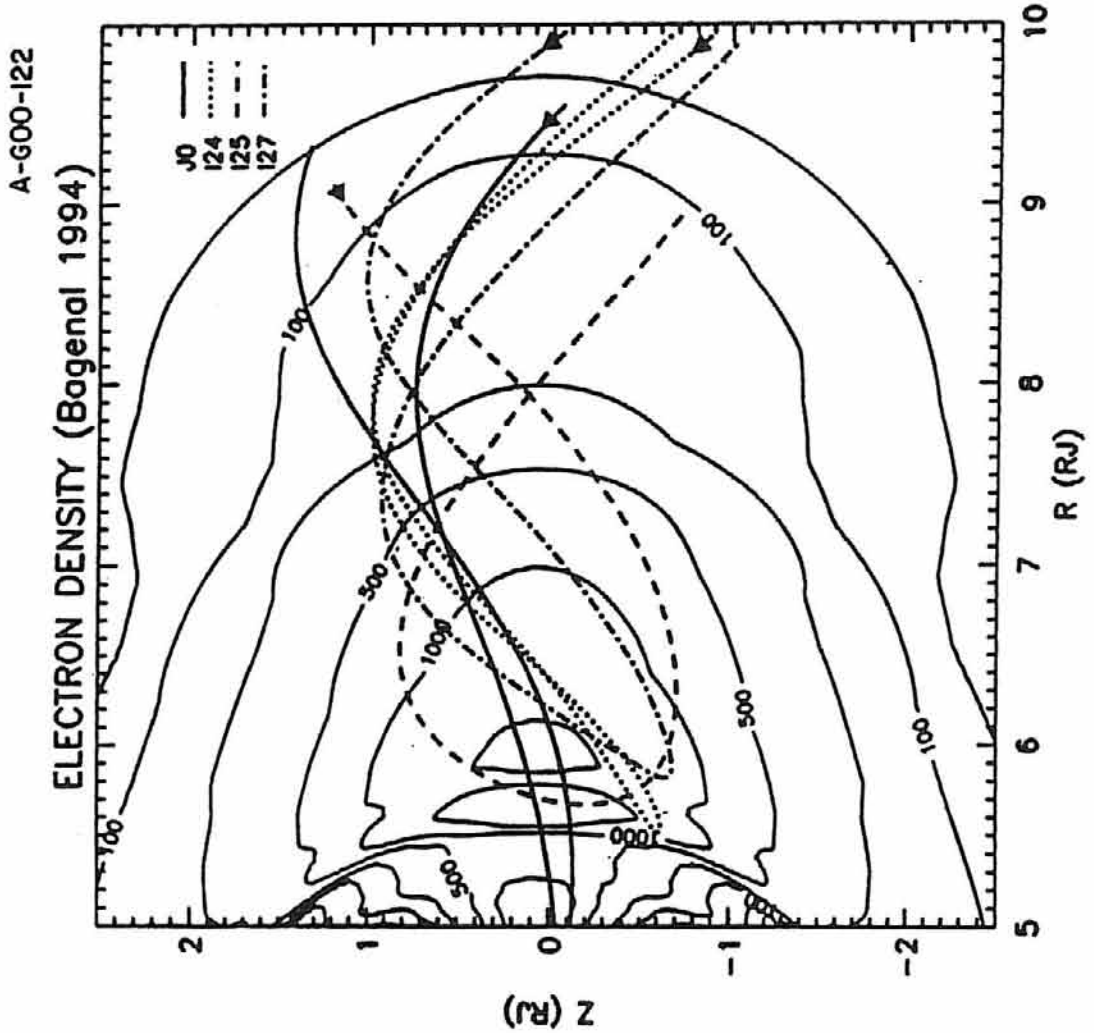
A-G00-I22
ELECTRON DENSITY (Bagenal 1994)
J0
I24
I25
I27
100
500
1000
Z (RJ)
R (RJ)
2
1
0
-1
-2
5
6
7
8
9
10

FIGURE 9. Power vs. Frequency Plot

In this plot the upper hybrid frequency can be seen between 10^5 and 10^6 Hz. This is an example of the type of plot that has been used to identify the upper hybrid frequency.

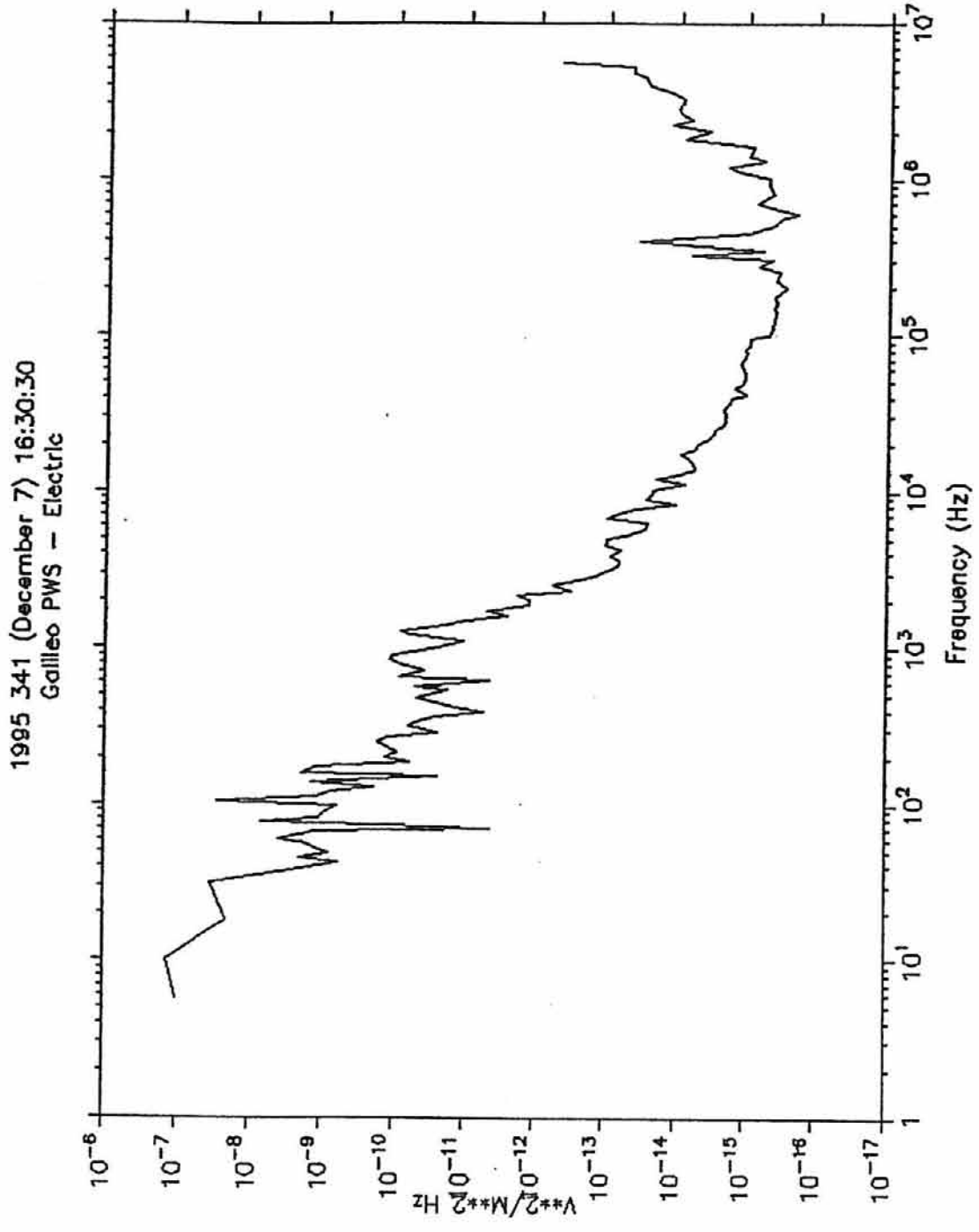
1995 341 (December 7) 16:30:30
Galileo PWS — Electric
V**2/M**2 Hz
Frequency (Hz)
10^-6
10^-7
10^-8
10^-9
10^-10
10^-11
10^-12
10^-13
10^-14
10^-15
10^-16
10^-17
1
10^1
10^2
10^3
10^4
10^5
10^6
10^7

FIGURE 10. Error Bar Plot for I24 Outbound

This shows the upper and lower limits, plotted as error bars, for the Plasma Wave Instrument determination of the electron density during outbound portion of the I24 pass. The error bars correspond to the upper and lower portion of the upper hybrid frequency signal in the spectrogram in figure 17.

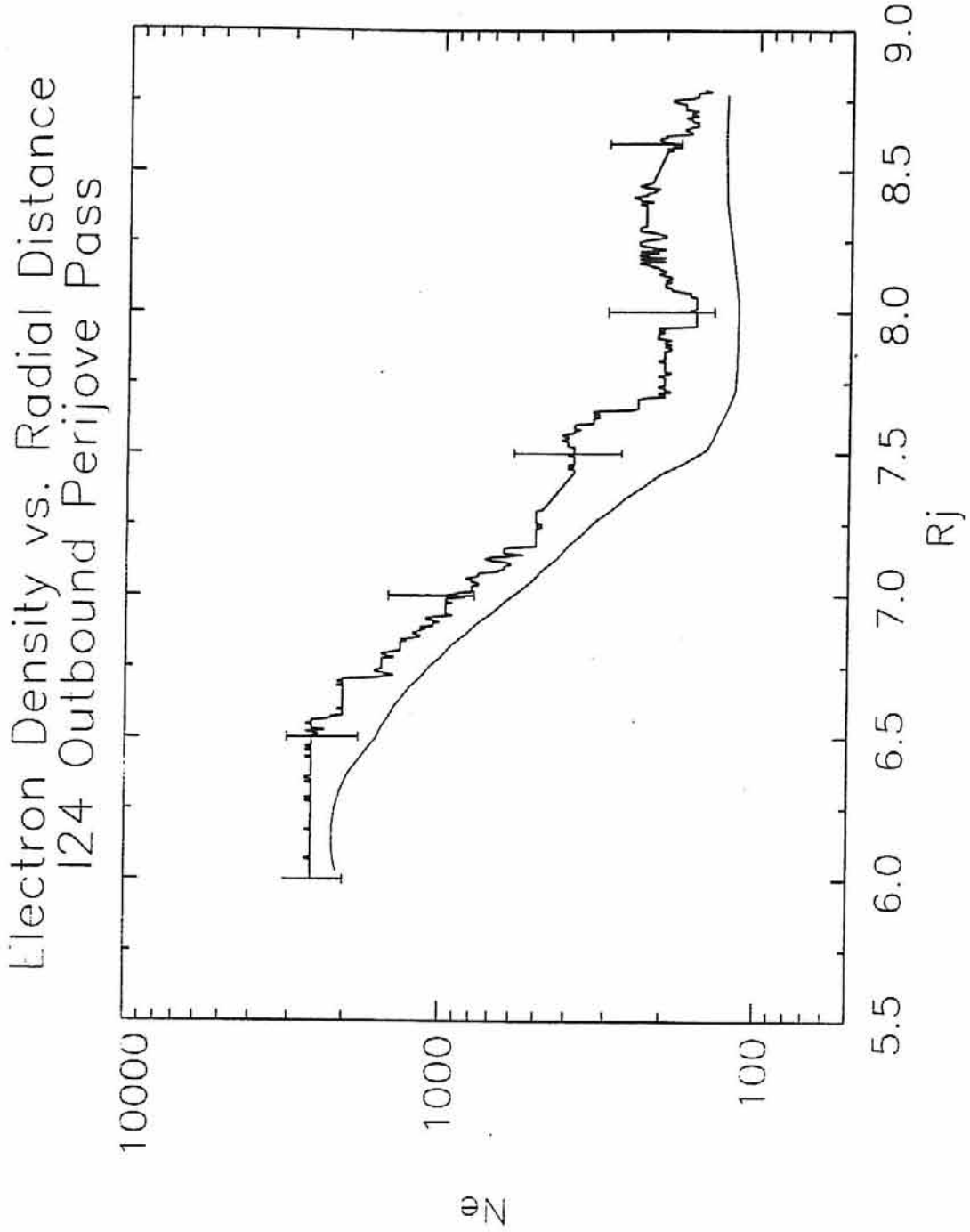
Electron Density vs. Radial Distance
124 Outbound Perijove Pass
10000
1000
100
N_e
5.5
6.0
6.5
7.0
7.5
8.0
8.5
9.0
Rj

FIGURE 11. Log Averaged Electron Density Ratio for Orbit J0

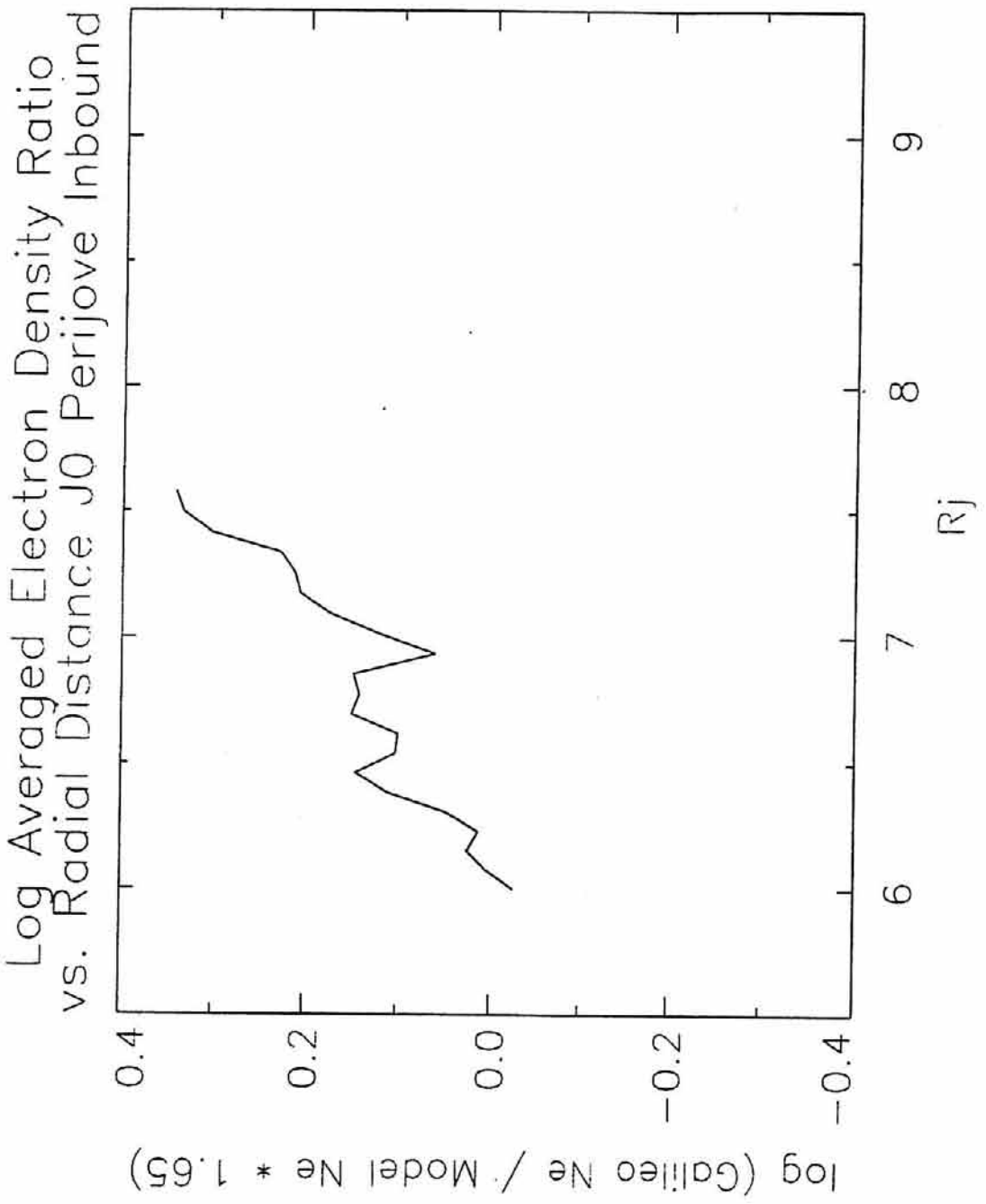
Log Averaged Electron Density Ratio
vs. Radial Distance J0 Perijove Inbound
log (Galileo Ne / Model Ne * 1.65)
0.4
0.2
0.0
−0.2
−0.4
6
7
8
9
Rj

FIGURE 12. Log Averaged Electron Density Ratio for I24 Outbound Pass

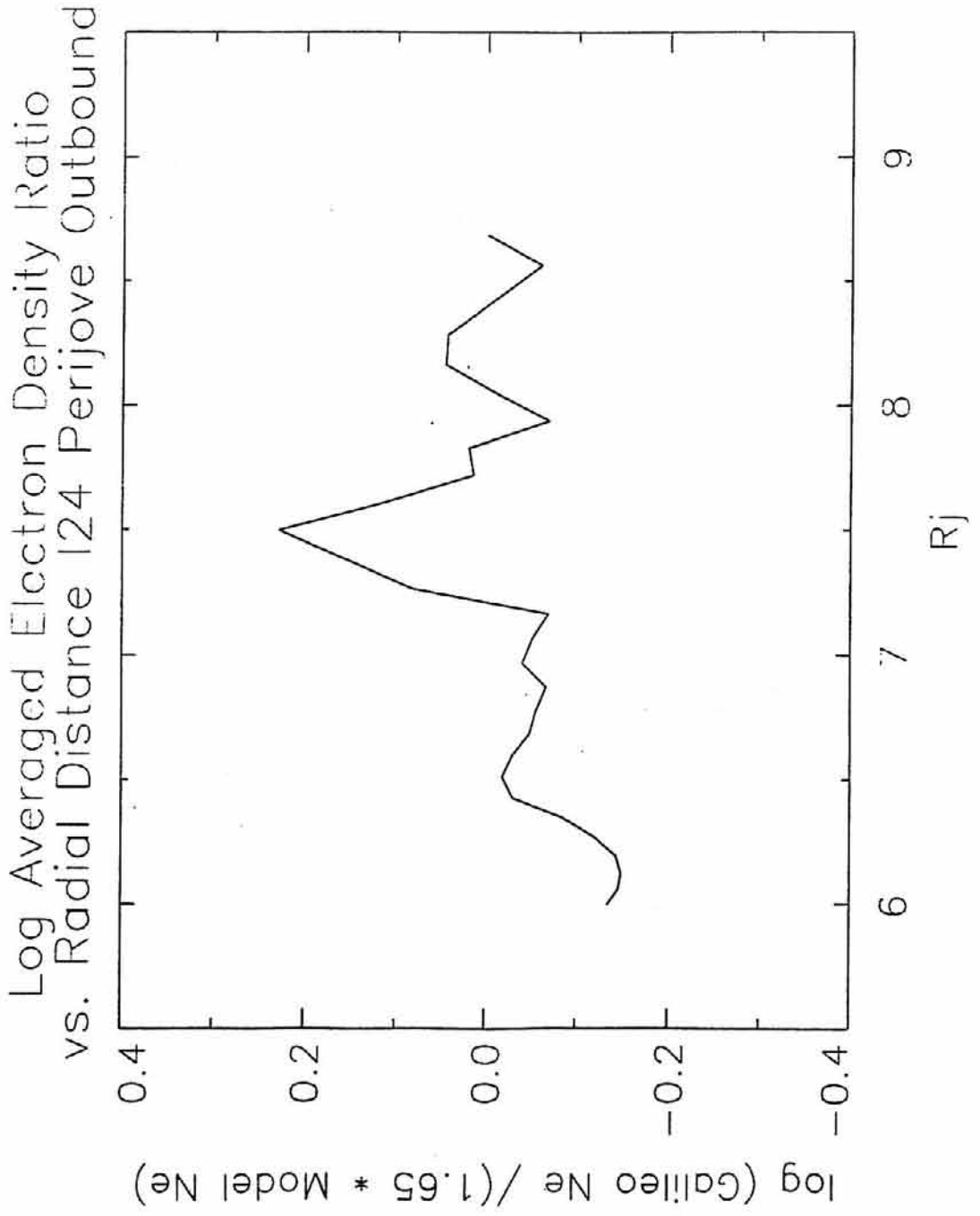
Log Averaged Electron Density Ratio
vs. Radial Distance I24 Perijove Outbound
log (Galileo Ne /(1.65 * Model Ne)
0.4
0.2
0.0
−0.2
−0.4
6
7
8
9
Rj

FIGURE 13. Log Averaged Electron Density Ratio for I25 Inbound Pass

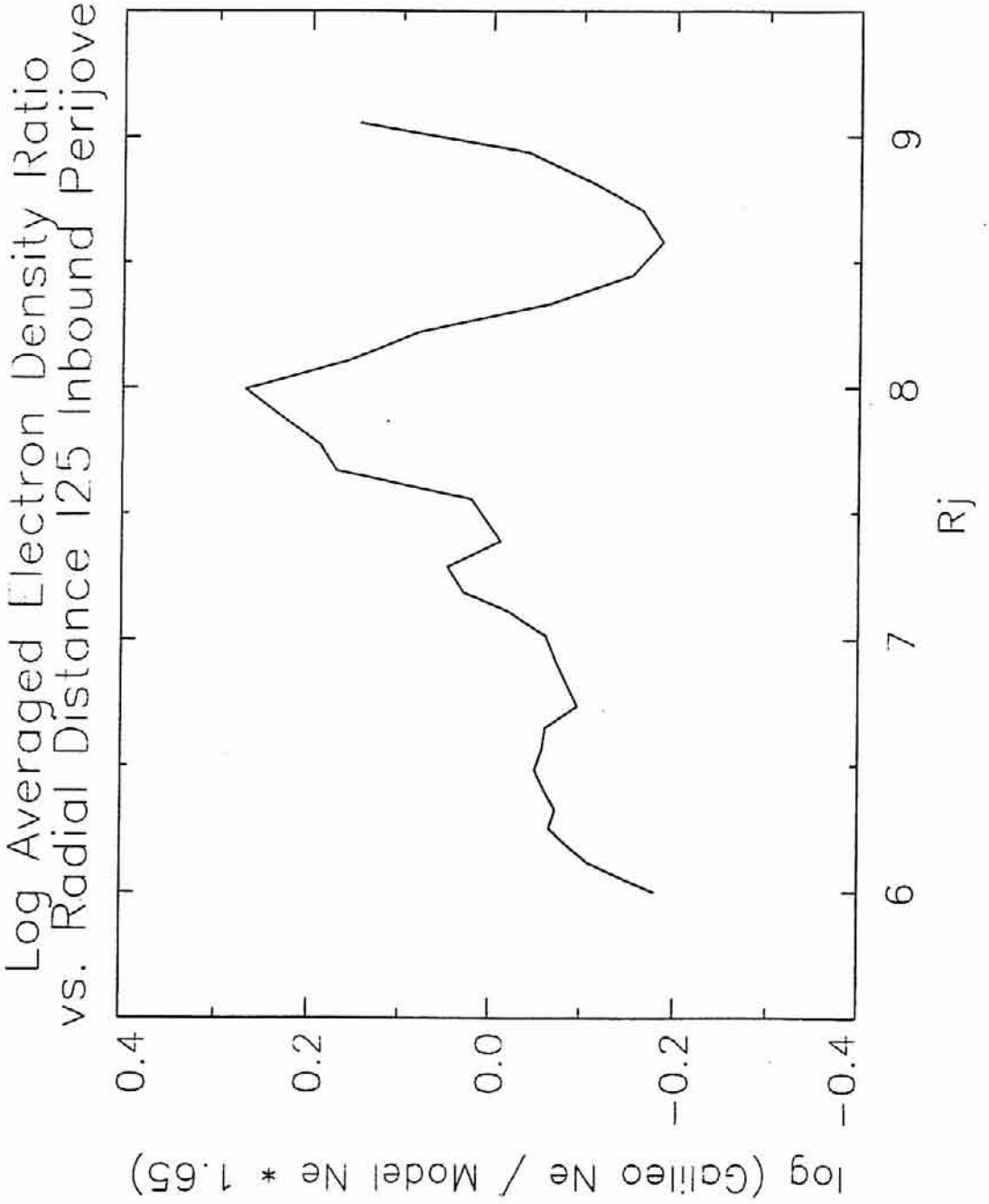
Log Averaged Electron Density Ratio
vs. Radial Distance I25 Inbound Perijove
log (Galileo Ne / Model Ne * 1.65)
0.4
0.2
0.0
−0.2
−0.4
6
7
8
9
Rj

FIGURE 14. Log Averaged Electron Density Ratio for I25 Outbound Pass

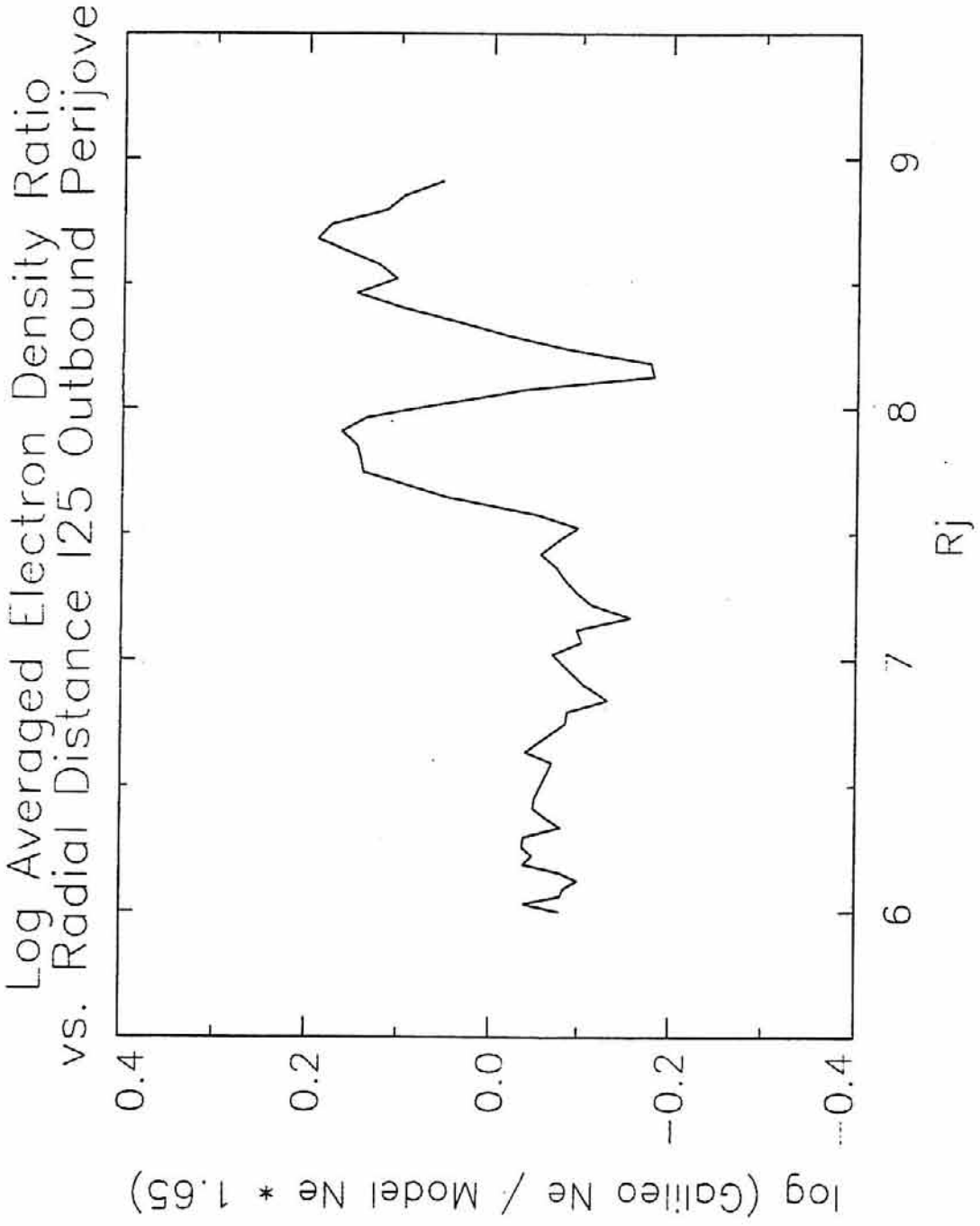
Log Averaged Electron Density Ratio
vs. Radial Distance I25 Outbound Perijove
log (Galileo Ne / Model Ne * 1.65)
0.4
0.2
0.0
−0.2
−0.4
6
7
8
9
Rj

FIGURE 15. Log Averaged Electron Density Ratio for I27 Inbound Pass

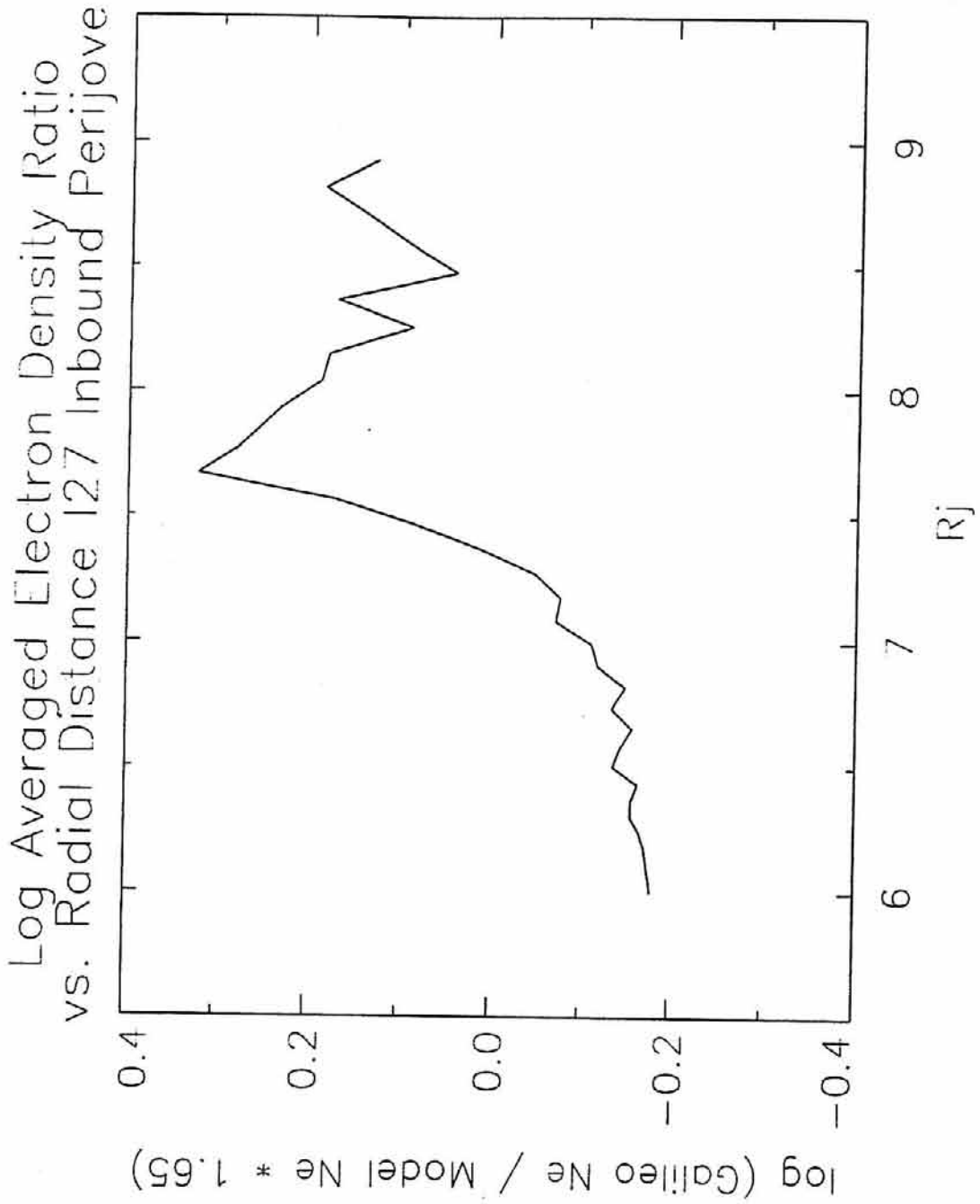
Log Averaged Electron Density Ratio
vs. Radial Distance I27 Inbound Perijove
log (Galileo Ne / Model Ne * 1.65)
0.4
0.2
0.0
−0.2
−0.4
6
7
8
9
Rj

Figure 16. Log Averaged Electron Density Ratio for I27 Outbound Pass

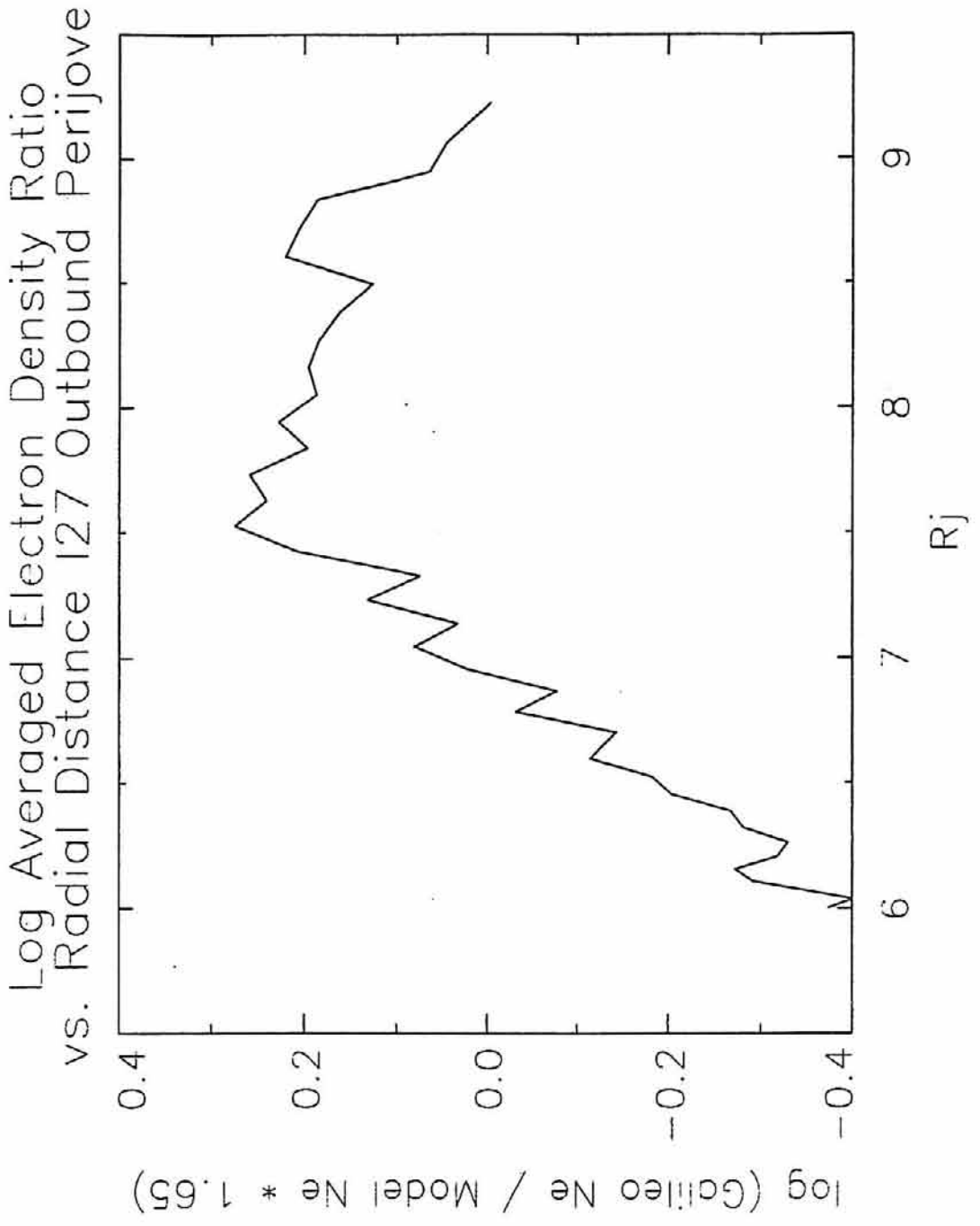
Log Averaged Electron Density Ratio
vs. Radial Distance I27 Outbound Perijove
log (Galileo Ne / Model Ne * 1.65)
0.4
0.2
0.0
−0.2
−0.4
6
7
8
9
Rj

Figure 17. Spectrogram for Orbit C23

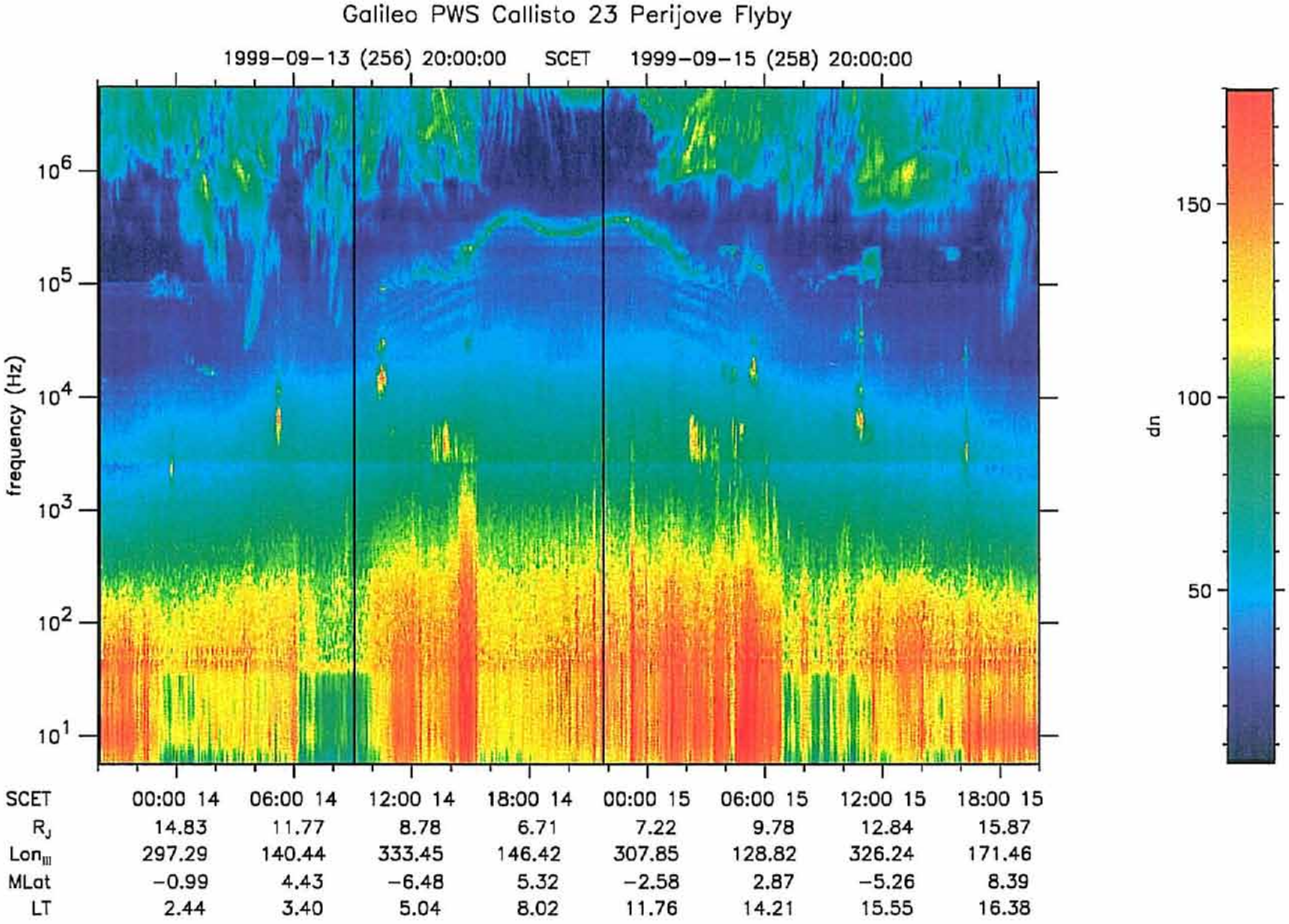
Galileo PWS Callisto 23 Perijove Flyby
1999-09-13 (256) 20:00:00 SCET 1999-09-15 (258) 20:00:00
frequency (Hz)
10^6
10^5
10^4
10^3
10^2
10^1
dB
150
100
50
SCET 00:00 14 06:00 14 12:00 14 18:00 14 00:00 15 06:00 15 12:00 15 18:00 15
R_J 14.83 11.77 8.78 6.71 7.22 9.78 12.84 15.87
Lon_{III} 297.29 140.44 333.45 146.42 307.85 128.82 326.24 171.46
MLat −0.99 4.43 −6.48 5.32 −2.58 2.87 −5.26 8.39
LT 2.44 3.40 5.04 8.02 11.76 14.21 15.55 16.38

Figure 18. Log Averaged Electron Density Ratio for C23 Orbit

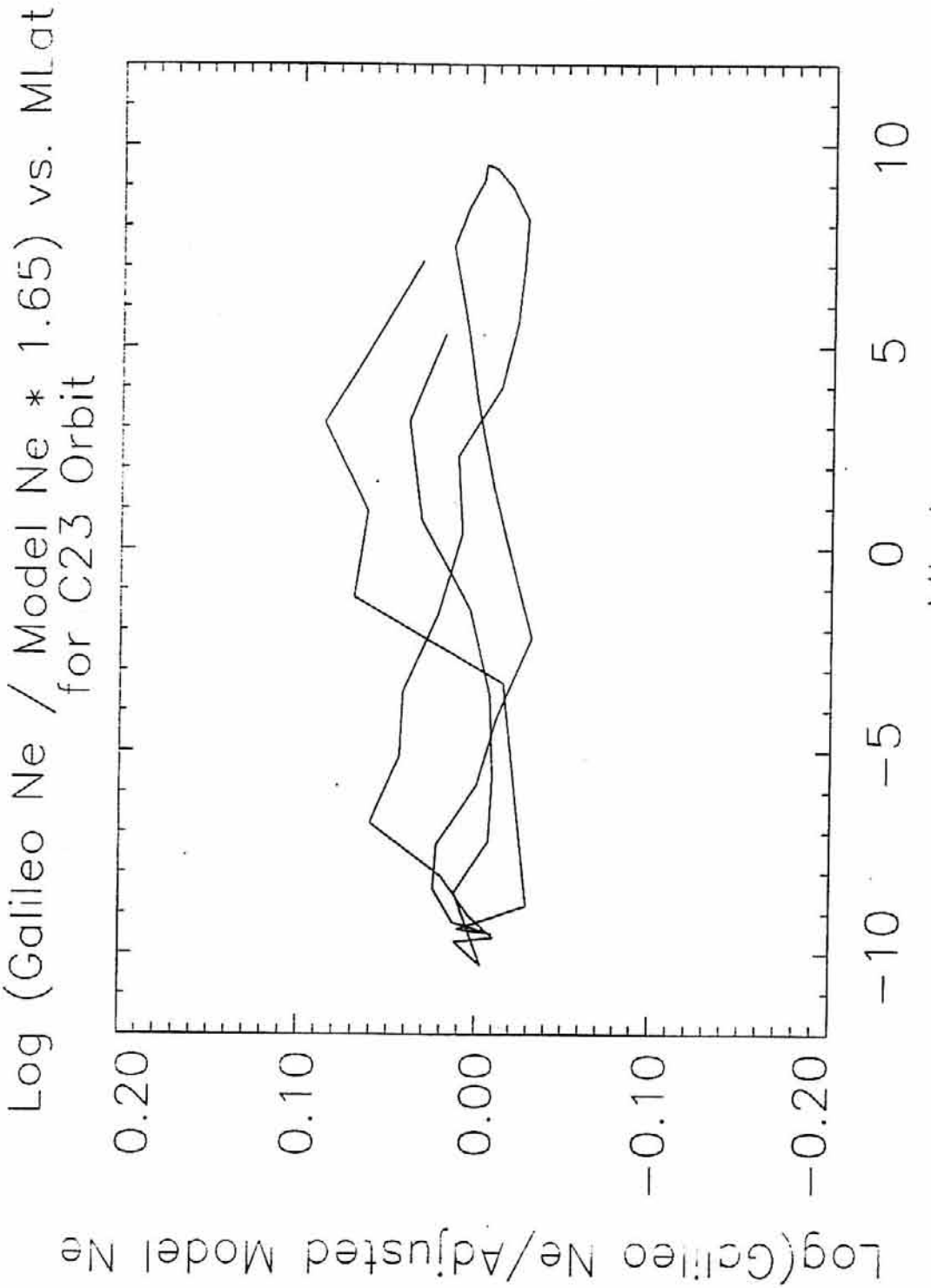
Log (Galileo Ne / Model Ne * 1.65) vs. MLat
for C23 Orbit
0.20
0.10
0.00
−0.10
−0.20
Log(Galileo Ne/Adjusted Model Ne
−10
−5
0
5
10
MLat

Figure 19. Log Averaged Electron Density Ratio for G29 Orbit

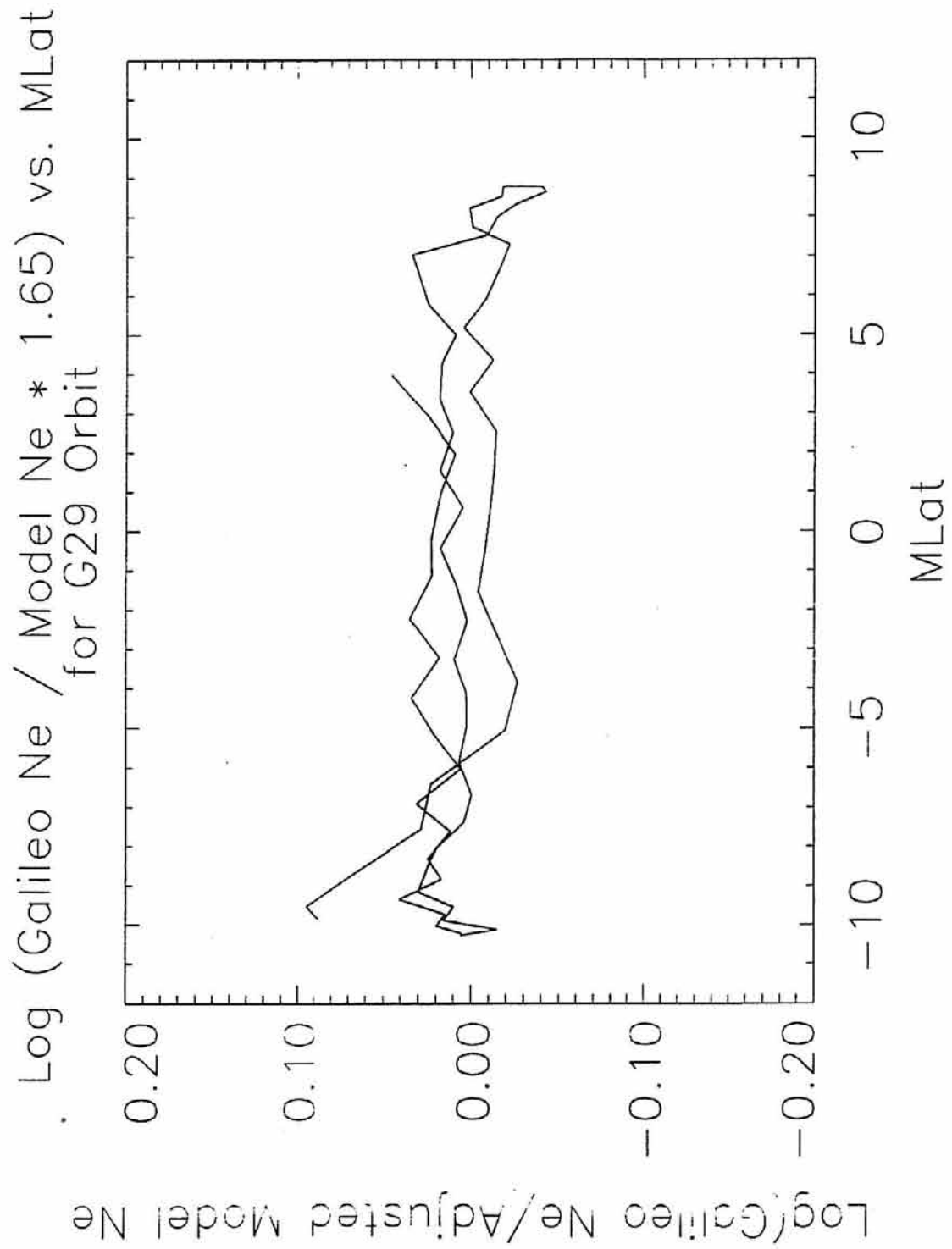
Log (Galileo Ne / Model Ne * 1.65) vs. MLat
for G29 Orbit
Log(Galileo Ne/Adjusted model Ne
0.20
0.10
0.00
−0.10
−0.20
−10
−5
0
5
10
MLat

APPENDIX I

PHYSICAL DATA FOR IO

Discovery:	Jan 7, 1610 by Galileo Galilei
Diameter (km):	3,630
Mass (kg):	8.94×10^{22}
Mass (Earth = 1)	0.014960
Surface Gravity (Earth = 1):	0.183
Mean Distance from Jupiter (km):	421,600
Mean Distance From Jupiter (R_J):	5.905
Mean Distance from Sun (AU):	5.20
Orbital period (days):	1.769138
Rotational period (days):	1.769138
Density (gm/cm^3)	3.57
Orbit Eccentricity:	0.0041
Orbit Inclination (degrees):	0.040
Orbit Speed (km/sec):	17.34
Escape velocity (km/sec):	2.56
Visual Albedo:	0.61
Typical Subsolar Temperature (K)	~135
Typical Hotspot Temperature (K)	~300
Surface Composition:	Sulphur

APPENDIX II

PHYSICAL DATA FOR JUPITER

Mass (kg)	1.90×10^{27}
Diameter (km)	142,800
Mean density (kg/m^3)	1314
Escape velocity (m/sec)	59500
Average distance from Sun (AU)	5.203
Rotation period (length of day in Earth hours)	9.8
Revolution period (length of year in Earth years)	11.86
Obliquity (tilt of axis in degrees)	3.08
Orbit inclination (degrees)	1.3
Orbit eccentricity (deviation from circular)	0.048
Mean surface temperature (K)	120 (cloud tops)
Visual geometric albedo (reflectivity)	0.44
Atmospheric components:	90% hydrogen, 10% helium, 0 .07% methane

NOTES

[i] The names of Jupiter's Galilean moons are, in order of their distance from Jupiter: Io, Europa, Ganymede and Callisto.

[ii] B. F. Burke, K. L. Franklin, *JGR*, **60**, 213-217 (1955).

[iii] E. K. Bigg, *Nature*, **203**, 1008-1010 (1964).

[iv] NASA has a website devoted to the Pioneer mission at: http://spaceprojects.arc.nasa.gov/Space_Projects/pioneer/PNhome.html

[v] I. Kupo, Y. Mekler, A. Eviatar, *Astrophysical J. Lett.*, **205**, 51-53 (1976).

[vi] R_J stands for Jovian Radii. It is a convenient and standard unit for describing positions in Jupiter's magnetosphere.

[vii] For a complete description of the Voyager mission and instrumentation see *Space Science Reviews*, **21**, 103-376, (1977). NASA maintains a Voyager website at: http://vraptor.jpl.nasa.gov/voyager/voyager.html

[xiii] S. J. Peale, P. Cassen, T. T. Reynolds, *Science* , **203** 892-894 (1979).

[ix] NASA operates a website for the Galileo mission at: http://www.jpl.nasa.gov/galileo/

[x] http://www.jpl.nasa.gov/ice_fire/europa.htm

[xi] In fact there are several models of Jupiter's magnetic filed. At a distance of 6 R_J from the planet, plasma parameters are not particularly sensitive to the various models. By 8 R_J perturbations from the plasma disk begin to significantly affect the magnetic field.

[xii] M. L. Kaiser, M. D. Desch, *GRL*, **7**, 389 (1980).

[xiii] Appendix I contains a list of physical data for Io.

[xiv] R. Prangé, *Planetary Torus*, Encyclopedia of the Solar System, J. H. Shirley, R. W. Fairbridge Eds., Chapman & Hall, New York (1977). Also, J. R. Spencer et al., *Science*, **288**, 1208-1210 (2000).

[xv] It has been estimated that over the age of the Solar System Io has lost 0.2% of its mass to Jupiter's magnetosphere. At this rate it will take Io another two trillion years, or 154 times the approximate age of the universe, to 'evaporate'.

[xvi] J. D. Sullivan, G. L. Siscoe, *In Situ Observations of Io Plasma Torus*, Satellites of Jupiter, D. Morrison Ed., University of Arizona Press, Tucson (1982).

[xvii] 1 eV = 11,600° K.

[xviii] J. D. Scudder, *JGR*, **86**, 8157-8179 (1981).

[xix] T. H. Stix, Waves in Plasmas, American Institute of Physics, New York (1992).

[xx] When I learned plasma physics the instructor used the analogy of mosquitoes hovering around a herd of elephants. The mosquitoes, representing the electrons, move back and forth very quickly around the elephants, representing the ions, which are too big and slow to respond.

[xxi] For a more complete description of this instrumentation see Gurnett et al., *Space Science Reviews*, **60**, 341-355 (1992).

[xxii] F. Bagenal, *JGR*, **99**, 11043-11062, (1994).

[xxiii] Of course the electron feels a gravitational force from Jupiter but at Io's average distance the centrifugal force is roughly 18 times stronger that the gravitational force.

[xxiv] J. D. Richardson, G. L. Siscoe, *JGR*, **86**, 8485-8490, (1981).

[xxv] D. E. Shemansky, *JGR*, **93**, 1773, (1988).

[xxvi] D. L. Book, *NRL Plasma Formulary*, Office of Naval Research, Washington , D. C. (1986).

[xxvii] A. J. Dessler, B. R. Sandel, *GRL*, **19**, 2099-2103, (1992) and J. S. Morgan, *Icarus*, **62**, 389, (1985).

[xxviii] Individual orbits are denoted by the first letter of the moon or planet of closest approach and the chronological orbit number. J0 is the 0^{th} orbit and it came nearest to Jupiter. I24 was the 24^{th} orbit and its closest approach was to Io, etc.

[xxix] The point of an orbit that is nearest to Jupiter is called the perijove point.

[xxx] The plots for all four orbits are on the same scale in both axes.

REFERENCES

Bagenal, F., *JGR*, **99**, 11043-11062, (1994).

Bagenal, F., Sullivan, J. D., *JGR*, **86**, 8447-8466, (1981).

Belcher, J. W., in Physics of the Jovian Magnetosphere, pp.68-105, Cambridge University Press,
New York (1983).

Gurnett, D. A. et al., *Space Science Reviews*, **60**, 341-355, (1992).

Murdin, P. Ed., Encyclopedia of Astronomy and Astrophysics, Nature Publishing Group, New York
(2001).

Peale, S. J., Cassen, P., Reynolds, R. T., *Science*, **203**, 892-894, (1979).

Scudder, J. D. et al., *JGR*, **86**, 8157-8179, (1981).

Shirley, J. H., Fairbridge, R. W. Eds., Encyclopedia of Planetary Sciences, Chapman & Hall, New York,
(1997).

Siscoe, G. L. , Summers, D., *JGR*, **86**, 8471-8479, (1981).

Sullivan, J. D., Siscoe, G. L., in Satellites of Jupiter, pp. 846-871, University of Arizona Press, Tucson,
(1982).

Thomas, N., *JGR*, **98**, 18737-18750, (1993).